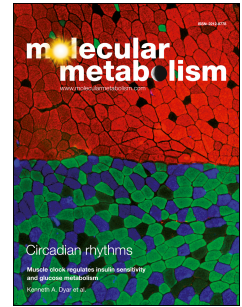


Journal Pre-proof

PPG neurons in the nucleus of the solitary tract modulate heart rate but do not mediate GLP-1 receptor agonist-induced tachycardia in mice

Marie K. Holt, Daniel R. Cook, Daniel I. Brierley, James E. Richards, Frank Reimann, Alexander V. Gourine, Nephtali Marina, Stefan Trapp



PII: S2212-8778(20)30098-3

DOI: <https://doi.org/10.1016/j.molmet.2020.101024>

Reference: MOLMET 101024

To appear in: *Molecular Metabolism*

Received Date: 24 March 2020

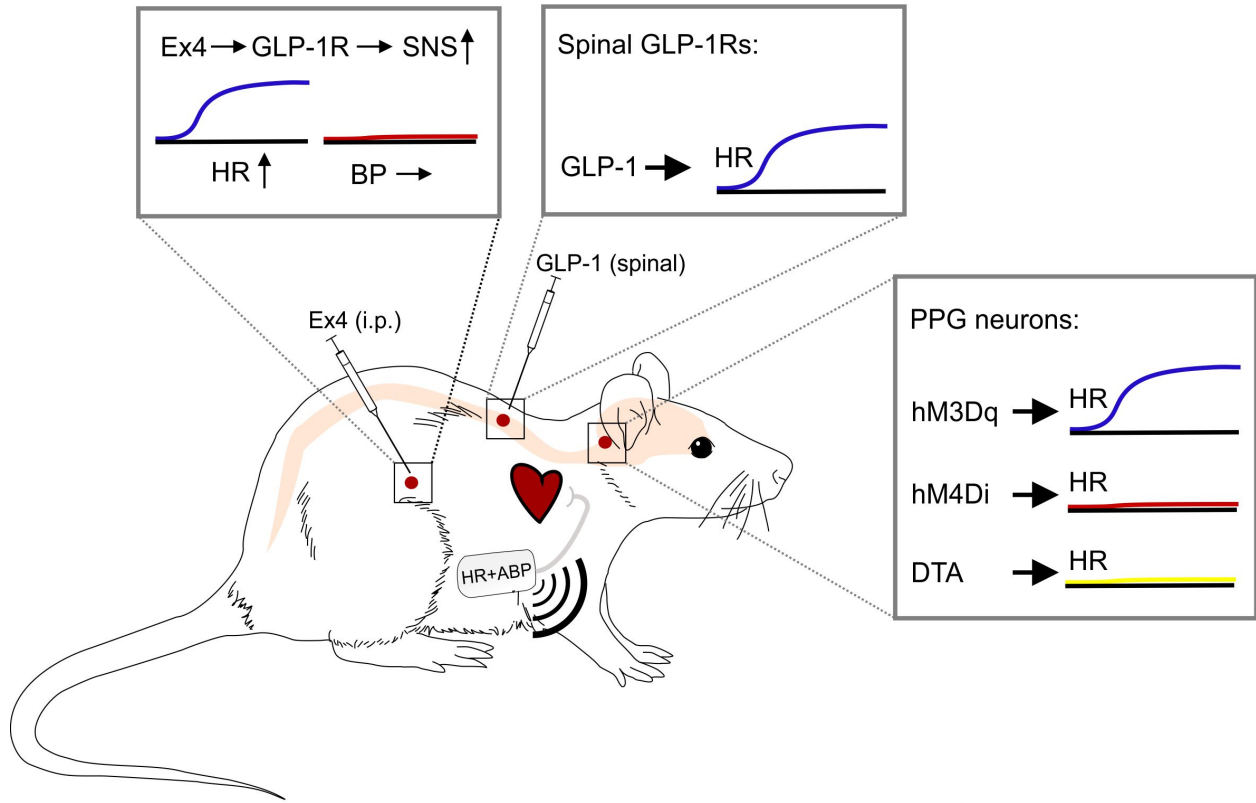
Revised Date: 13 May 2020

Accepted Date: 13 May 2020

Please cite this article as: Holt MK, Cook DR, Brierley DI, Richards JE, Reimann F, Gourine AV, Marina N, Trapp S, PPG neurons in the nucleus of the solitary tract modulate heart rate but do not mediate GLP-1 receptor agonist-induced tachycardia in mice, *Molecular Metabolism*, <https://doi.org/10.1016/j.molmet.2020.101024>.

This is a PDF file of an article that has undergone enhancements after acceptance, such as the addition of a cover page and metadata, and formatting for readability, but it is not yet the definitive version of record. This version will undergo additional copyediting, typesetting and review before it is published in its final form, but we are providing this version to give early visibility of the article. Please note that, during the production process, errors may be discovered which could affect the content, and all legal disclaimers that apply to the journal pertain.

© 2020 The Author(s). Published by Elsevier GmbH.



Journal ↑

PPG neurons in the nucleus of the solitary tract modulate heart rate but do not mediate GLP-1 receptor agonist-induced tachycardia in mice

Marie K. Holt^{1a}, Daniel R. Cook¹, Daniel I. Brierley¹, James E. Richards¹, Frank Reimann², Alexander V. Gourine¹, Nephthali Marina^{1*} & Stefan Trapp^{1*}

¹*Centre for Cardiovascular and Metabolic Neuroscience, Department of Neuroscience, Physiology & Pharmacology, UCL, London, UK*

²*Wellcome Trust/MRC Institute of Metabolic Science (IMS), Addenbrookes Hospital, University of Cambridge, Cambridge, UK*

^aCurrent address: Florida State University, Department of Psychology and Program in Neuroscience, Tallahassee, Florida, USA

* correspondence should be sent to either s.trapp@ucl.ac.uk or n.marina@ucl.ac.uk

Address for correspondence during submission:

Dr Stefan Trapp

Centre for Cardiovascular and Metabolic Neuroscience

Department of Neuroscience, Physiology and Pharmacology

University College London

London WC1E 6BT

UK

Tel: ++44 (0)207 6794 6094

Email: s.trapp@ucl.ac.uk

Abstract

Objective Glucagon-like peptide-1 receptor agonists (GLP-1RAs) are used as anti-diabetic drugs and are approved for obesity treatment. However, GLP-1RAs also affect heart rate (HR) and arterial blood pressure (ABP) in rodents and humans. While activation of GLP-1 receptors (GLP-1R) is known to increase HR, the circuits recruited are unclear, and in particular it is unknown whether GLP-1RAs activate preproglucagon (PPG) neurons, the brain source of GLP-1, to elicit these effects.

Methods We investigated the effect of GLP-1RAs on heart rate in anaesthetized adult mice. In a separate study, we manipulated the activity of nucleus tractus solitarius (NTS) PPG neurons (PPG^{NTS}) in awake, freely behaving transgenic Glu-Cre mice implanted with biotelemetry probes and injected with AAV-DIO-hM3Dq:mCherry or AAV-mCherry-FLEX-DTA.

Results Systemic administration of the GLP-1RA Ex-4 increased resting HR in anaesthetized or conscious mice, but had no effect on ABP in conscious mice. This effect was abolished by β -adrenoceptor blockade with atenolol, but unaffected by the muscarinic antagonist atropine. Furthermore, Ex-4-induced tachycardia persisted when PPG^{NTS} neurons were ablated, and Ex-4 did not induce expression of the neuronal activity marker cFos in PPG^{NTS} neurons. PPG^{NTS} ablation or acute chemogenetic inhibition of these neurons via hM4Di receptors had no effect on resting HR. In contrast, chemogenetic activation of PPG^{NTS} neurons increased resting HR. Furthermore, application of GLP-1 within the subarachnoid space of the middle thoracic spinal cord, a major projection target of PPG neurons, increased HR.

Conclusions These results demonstrate that both systemic application of Ex-4 or GLP-1 and chemogenetic activation of PPG^{NTS} neurons increases HR. Ex-4 increases the activity of cardiac sympathetic preganglionic neurons of the spinal cord without recruitment of PPG^{NTS} neurons, and thus likely recapitulates the physiological effects of PPG neuron activation. These neurons thus do not play a significant role in controlling resting HR and ABP, but are capable of inducing tachycardia, and so are likely involved in cardiovascular responses to acute stress.

Keywords (max 6)

GLP-1, cardiovascular function, PPG neurons, biotelemetry, sympathetic outflow, chemogenetics

1. Introduction

Glucagon-like peptide-1 (GLP-1) is best known as an incretin, that is released from the gut into the bloodstream postprandially and enhances insulin secretion. Based on that function GLP-1 receptor agonists (GLP-1RAs), such as exendin-4 (Ex-4), are in clinical use to treat type 2 diabetes mellitus. However, both animal studies and clinical observations have established that GLP-1RAs have cardiovascular effects, including an increase in heart rate (HR)[1-7]. Despite the magnitude of these effects being typically modest, the high incidence of cardiovascular disease as comorbidity of type 2 diabetes makes this observation pertinent and analysis of the underlying mechanisms worthwhile.

Arguably, it seems counterintuitive that a gut peptide involved in blood glucose control should be involved in cardiovascular control. However, GLP-1 is also produced within the brain, and there it is involved primarily in the regulation of food intake, but also in stress responses [8-16]. In fact, food intake, anxiety-like behaviour, corticosterone levels, and sympathetic activity are all modulated in response to challenges to survival, including acute stress [17-19] with GLP-1 being implicated in the modulation of all these functions. Within the brain, GLP-1 suppresses food and water consumption, decreases reward, drives anxiety-like behaviour, activates the hypothalamic-pituitary-adrenal (HPA) axis, and increases HR and arterial blood pressure (ABP) [20-24].

This raises numerous questions. Firstly, where are the relevant populations of GLP-1 receptors (GLP-1Rs) for cardiovascular control located? Are these targets for brain-derived, rather than gut-derived, GLP-1? And if so, does that have consequences for the clinical use of current GLP-1RAs, or for the use of future drugs designed to potentiate the activity of GLP-1-producing neurons in the brain? While it is now well established that both systemically and centrally applied GLP-1RAs can increase HR, the neural circuits involved remain controversial [5, 6, 22, 24-28]. The parasympathetic [2, 3, 5, 25] and sympathetic [1, 13, 24, 29] nervous systems have both been implicated in these effects, but the contribution of endogenous brain-derived GLP-1 to the modulation of HR and ABP remains inconclusive. The only observation related to endogenous GLP-1 stems from Barragan et al. (1999), who found no effect of intracerebroventricular (i.c.v.) infusion of the GLP-1R antagonist, Ex-9, on HR and ABP [3]. More recently, Ghosal et al. demonstrated that the cardiovascular response to restraint stress was reduced in mice lacking GLP-1R in *Sim1* neurons in the paraventricular nucleus of the hypothalamus (PVN) [13], adding to a wealth of evidence pointing to a role for brain GLP-1 in central responses to stressful stimuli [8-13, 20, 30-34].

The main source of GLP-1 within the brain are preproglucagon (PPG) neurons of the lower brainstem [8]. The effect induced by i.c.v. delivery of GLP-1RAs likely recapitulates a physiological role of PPG neurons in cardiovascular control. In support of this, PPG neurons have been found to project to the presympathetic nuclei of the PVN and the rostral ventrolateral medulla (RVLM) [35, 36] as well as directly to sympathetic preganglionic neurons (SPN) located in the intermediolateral cell column (IML) and central autonomic area (CAA) of the spinal cord [37]. GLP-1Rs have been identified on both sympathetic neurons in the PVN, RVLM, and lamina X of the spinal cord, as well as in cardiac vagal preganglionic neurons of the nucleus ambiguus and dorsal motor nucleus of the vagus [38-40].

We recently showed that selective activation of PPG^{NTS} neurons with chemogenetic methods produces a suppression of food consumption, and that their activity is necessary for stress-induced suppression of feeding [8]. Here we build on those findings by investigating the effect of systemic GLP-1R activation on HR, the involvement of PPG^{NTS} neurons in these effects, and the physiological role of PPG^{NTS} neurons in cardiovascular control. We demonstrate that, in the mouse, GLP-1R activation has no effect on resting ABP, but elicits significant tachycardia, which is mediated by an increase in sympathetic outflow. Direct application of GLP-1 onto the thoracic spinal cord was sufficient to elicit robust increases in HR, and ablation of PPG^{NTS} neurons did not prevent tachycardia following systemic administration of GLP-1. Finally, we show through chemogenetic activation that PPG^{NTS} neurons have the capacity to increase HR, but also demonstrate through both chemogenetic inhibition and ablation that PPG^{NTS} neuronal activity do not provide tonic control of cardiac chronotropy under resting conditions.

2. Materials and Methods

2.1. Animals

We used adult Glu-Cre [41-43] and Glu-YFP [44] mice of either sex on a C57Bl6 background. Mice were usually group-housed and kept on a 12 h dark/light cycle with water and chow available *ad libitum*. Experiments were conducted in accordance with the U.K. Animals (Scientific Procedures) Act, 1986, with appropriate ethical approval.

2.2. Anaesthetized preparations

Naïve 13-26-week-old Glu-YFP (or Glu-Cre, where they underwent previous stereotaxic viral transduction) mice were anaesthetized with urethane (1.3g/kg, intraperitoneally (i.p)),

following 4% isoflurane induction) or urethane (650mg/kg) + alpha-chloralose (50mg/kg) intravenously. The trachea was cannulated with a plastic tube and core body temperature was kept at 37 °C throughout the experiment with a servo-controlled heating pad. The femoral vein was cannulated for the infusion of drugs. The depth of anaesthesia was monitored using stability of HR, corneal reflexes and absence of flexor responses to paw□pinch.

2.2.1. Stereotaxic injections

All stereotaxic injections were performed on 9-22-week-old Glu-Cre mice. Animals were anaesthetized with a mixture of ketamine hydrochloride (50mg/kg; intramuscular (i.m.)) and medetomidine (1mg/kg; i.m.) or 1.5-2.5% isoflurane and the skull was fixed in a stereotaxic frame. A core temperature of 37°C was maintained throughout the procedure using a heating mat. The nose of the mouse was pushed downwards, creating a right angle between the nose and the neck to expose part of the brainstem normally covered by the cerebellum. A longitudinal incision was made from the occipital bone to the first vertebra. Obex was exposed by parting overlying muscle layers and the atlanto-occipital membrane was pierced using a 30G needle. Adeno-associated viral vectors (AAV; Table 1) were injected bilaterally (250 nl) using the following coordinates from obex: 0.50 mm lateral; 0.10 mm rostral; 0.35 mm ventral. Anaesthesia was reversed with Antisedan (2.5 mg/kg; i.m.) and mice received buprenorphine (0.5 mg/kg; subcutaneous (s.c.)) for pain relief and 100 µl sterile saline (s.c.) for fluid support. Animals were left to recover in a 34°C chamber until fully awake and experiments commenced 2-4 weeks after viral gene transfer.

2.2.2. ECG recordings in anaesthetized mice

Needle electrodes were inserted subcutaneously in a lead II configuration (bilaterally at the anterior axillary lines with the ground electrode inserted in the left or right lower limb) to record surface electrocardiogram (ECG). The signal was recorded through a high impedance headstage (NL 100, Neurolog; Digitimer Ltd, UK), sampled at 2 kHz, amplified \times 50–100, and filtered to a bandwidth between 5 and 100 Hz with 50 Hz notch filtering). ECG traces were recorded in Spike2 software (CED) and HR was derived from the R-R interval of the ECG. The frequency of the R wave was averaged over 5 seconds and plotted as a graph in beats per minute.

HR data were exported from Spike2 into Microsoft Excel. Baseline HR was defined as the mean HR over a 10-minute dataset prior to the start of the experiment. At each timepoint mean HR was extracted by averaging the HR at timepoint \pm 30s to remove the effect of any

possible interference in the trace. Drug-induced changes in mean level of activity were normalized with respect to the baseline level (Δ HR).

Drugs were delivered via i.v. or i.p. injections, or directly onto the exposed thoracic spinal cord. For application directly onto the spinal cord, the middle thoracic vertebrae were exposed and the T8 lateral processes were bilaterally clamped and fixed to a stereotaxic spinal unit. The ligamentum flavum was removed between T7 and T8 and the dura mater was incised with a 21 G needle. Cerebrospinal fluid outflow was used as indicator of access to the subarachnoid space and correct exposure of the dorsal surface of the thoracic spinal cord.

2.3. Awake preparations

2.3.1 Tail-cuff blood pressure measurements

ABP and HR of ten 7-10-week-old male Glu-YFP mice were measured using the CODA high throughput volume-pressure recording (VPR) tail-cuff system (Kent Scientific). Mice were placed in a perforated plexiglass tube, fixed tightly in place, and placed on a 32°C heat pad. An occlusion cuff and a VPR cuff were placed over the tail and 25 measurement cycles were taken. Average HR and ABP were calculated from a minimum of ten successful measurements.

2.3.2 Biotelemetry probe implantation and stereotaxic injections

Biotelemetry was used to monitor ABP and HR in conscious, freely-moving animals. Male 7-10-week-old Glu-Cre mice were anaesthetized with 1.5-2.5% isoflurane and the left common carotid artery was exposed. A gel-filled catheter connected to a pressure transmitter (TA11-PA-C10, Data Science International) was inserted and secured with sutures. The transmitter was placed subcutaneously on the abdominal wall and the incision was closed using 6-0 absorbable suture. The animals received buprenorphine (0.05 mg/kg per day, subcutaneous) and were allowed to recover for at least seven days before ABP recordings started. All mice were kept in individual cages after implantation. 2-4 weeks after telemetry implantation mice were subjected to stereotaxic injection of AAVs, as described under 2.2.1.

2.3.3. Biotelemetry recordings

ABP and activity was recorded continuously for 24 h in conscious freely-moving mice. Data were acquired at a sampling rate of 500-1000 Hz and these raw data were pre-processed using a proprietary algorithm (embedded in Dataquest ART software; Data Science

International) to calculate HR and mean arterial blood pressure (MAP) in 10s time bins. These data were subsequently exported to Microsoft Excel and The R Project for Statistical Computing, R 3.3.1 (R Core Team 2016) for further analysis.

Continuous traces displaying HR or MAP from a single representative mouse over extended periods of time were smoothed using a running average to be able to recognise trends. Each data point (every 10s) is the average of the preceding period of data points. The length of this period is given in the individual figure legend.

Plotting the distribution of HR values for individual mice (Fig. S1B,C) revealed that HR values (and MAP; not shown) are not normally distributed, but rather form a bimodal distribution comprising of two unimodal, non-normal distributions which can be separated based on activity levels (Fig S1B,C). Consequently, the median, rather than the mean, for each mouse is used as a measure of resting or active HR or MAP. For population data the mean \pm sem of these median values is calculated and displayed. One individual factor that strongly correlates with HR is activity (Fig. S1C). As a result, HR and MAP were analysed separately during rest and during activity. To determine resting values for HR and MAP, Dataquest ART datasets from across the 24-hour recording period were screened for periods of inactivity of at least 10 mins. Since HR and MAP do not return to baseline immediately following periods of locomotor activity, the first three minutes of every 10 min period of inactivity were disregarded in order to avoid any contamination of HR and MAP from recent activity. HR and MAP values from the last seven minutes of these inactive periods were combined and the median determined as a measure of resting heart rate for each mouse.

2.3.3.1 Cardiovascular effects of Ex-4 in freely-moving mice

Four hours into the light phase mice received an i.p injection of either GLP-1 (100 μ g/kg), Ex-4 (10 μ g/kg) or saline. For studies using sympathetic blockade, mice were injected with the β 1-adrenoreceptor antagonist atenolol (2 mg/kg, i.p.) three hours and 45 mins into the light phase followed 15 mins later by an injection of Ex-4 or vehicle (saline). All injections were delivered in a volume of 100 μ l and experiments were performed using a within-subjects counterbalanced design, with a minimum 48-hour washout period between experiments. The doses of GLP-1 (100 μ g/kg) and Ex-4 (10 μ g/kg) were chosen based on previous studies reporting significant effects on food intake [45-49].

2.3.3.2 Pharmacogenetic activation of PPG^{NTS} neurons

EGFP- or hM3Dq-expressing male Glu-cre mice were injected 7.5 hours into the light phase with clozapine-N-oxide (CNO, 2 mg/kg in 5 ml/kg saline; i.p.) or with saline only in a within-subjects counterbalanced design. HR, MAP and level of activity were recorded over the following 24 hours, with a minimum 48-hour washout period between experiments.

2.3.3.3 Cardiovascular effects of PPG^{NTS} neuron ablation

For this longitudinal study, baseline HR, MAP and level of activity were recorded and two weeks later male Glu-Cre mice were stereotaxically injected into the NTS with either AAV8-mCherry-FLEX-DTA or AAV1/2-FLEX-Perceval as control. HR and MAP were recorded again four and six weeks after viral gene delivery. At nine weeks, DTA and control animals received i.p. injections of saline and 10 µg/kg Ex-4 as described above.

2.4. Histological reconstruction

At the end of the experiments, mice were transcardially perfused with 0.1 M phosphate buffered saline (PB) followed by 4% formaldehyde in 0.1 M PBS and coronal brainstem sections (30 µm) were immunostained for the fluorescent reporters mCherry, EGFP, or Perceval as markers for successful targeting of the PPG^{NTS} neurons, as described previously [8, 42]. Details of antisera used are given in Table 1. All mice were found to be expressing the expected transgene. DTA ablation of PPG neurons was confirmed by absence of GCaMP3 immunoreactive cell bodies in the NTS, together with widespread mCherry expression, signifying viral spread. Transduction with hM3Dq and hM4Di was confirmed by mCherry expression. Selective Cre-dependent expression of all viruses in PPG^{NTS} neurons used in the present study was demonstrated previously [8] and confirmed by examination of co-expression of virally-encoded mCherry and the transgenic label GCaMP3. From a subset of sections (n=3 mice) this was quantified as 10.2% of Glu-Cre cells not transduced by the virus, and 13.5% of virus-transduced cells not expressing GCaMP3. This confirmed >85% co-expression.

2.5. cFos expression in PPG neurons

12-16-week-old Glu-YFP mice of either sex received an i.p. injection of saline or Ex-4 (10 µg/kg) four hours into the light phase and 90 min later were transcardially perfused with 0.1 M phosphate buffered saline followed by 4% formaldehyde in 0.1 M phosphate buffer. Brainstem tissue was processed and stained for cFOS and YFP as described before [8]. Details of antisera and dilutions are given in Table 1.

2.6. Statistics

Data were analysed for statistical significance as detailed in figure legends using Student's t-test, one-way within-subjects or two-way within-subjects / mixed-model ANOVA (with the Greenhouse-Geisser correction applied where necessary), or non-parametric equivalents as appropriate. Significant one-way ANOVA tests were followed by pairwise comparisons with Tukey's or Dunnett's correction for multiple comparisons. For two-way ANOVA, simple main effects were reported, or significant treatment x time interactions were followed by analysis of treatment effects at each time point with Sidak's correction for multiple comparisons.

3. Results

3.1. Systemic exendin-4 increases heart rate in freely behaving and anaesthetized mice

HR, MAP, and activity level were measured in awake, freely behaving male mice using implantable biotelemetry probes (Fig S1A). Conscious mice had resting HR of 505 ± 12 bpm, and resting MAP of 103 ± 1 mmHg.

Injection of 100 μ l saline i.p. led to a rapid increase in HR (Fig. 1A,B) and MAP (Fig 1C) as expected due to handling of the mouse and noxious stimulation induced by the injection. Both HR and MAP returned to baseline over 30 min and continued to fluctuate as normal with more frequent returns to high values during the dark phase when the mice are more active (Fig 1A-C, S1A,C). Similarly, i.p. injection of 100 μ g/kg GLP-1 caused a transient increase in HR, which returned to baseline within 30 mins (Fig 1A). In contrast, i.p. injection of the long-acting GLP-1 analogue Ex-4 (10 μ g/kg) led to a sustained increase in HR over the remainder of the light phase (Fig 1A,B), whereas MAP was unaffected by systemic GLP-1R activation (Fig 1C).

Ex-4 increased the minimum level of HR, whilst peak rates remained unchanged, suggesting the effect was mainly on resting HR (Fig. 1A). Consequently, resting HRs were calculated over 1h before (Zeitgeber 2-3 h) and after (Zeitgeber 5-6 h) drug treatments. Ex-4 (10 μ g/kg, i.p.) significantly increased resting HR (Fig 1D,E), corroborating previous findings that GLP-1R activation increases mean HR [24, 25, 50], without affecting activity levels (Fig S1D-F). There was no effect of saline or GLP-1 on resting HR during the time window analysed.

Given that Ex-4 significantly increased resting HR and since the effects of GLP-1 were potentially masked by the cardiovascular stress response, we explored the effects of systemic GLP-1R activation under anaesthesia, when stress is not a confounding factor. Infusion of GLP-1 (100 µg/kg; i.v.) and two doses of Ex-4 (10 and 100 µg/kg; i.p.) significantly increased HR with comparable amplitudes (Fig 1F,G). Interestingly, the effect of 10 µg/kg Ex-4 was substantially smaller under anaesthesia than in conscious mice (Fig 1E,G). We reasoned that urethane anaesthesia might increase sympathetic tone [51] and thus reduce the scope for GLP-1R activation to increase HR via an increase in sympathetic outflow. This hypothesis was tested by applying Ex-4 (i.p.; 10 µg/kg) in mice anaesthetized with urethane (650 mg/kg) + α -chloralose (50 mg/kg), an anaesthetic regime which maintains a lower sympathetic tone [51]. Resting HR under these conditions was significantly lower than under urethane alone and close to the resting HRs recorded with biotelemetry in conscious mice (Fig S2A) and i.p. injection of Ex-4 (10 µg/kg) triggered HR responses that were almost three times greater than under urethane alone (Fig. 1H and 1G, respectively).

3.2. Systemic GLP-1R activation increases heart rate via the sympathetic nervous system

To determine if the increase in HR by Ex-4 is due to increased sympathetic outflow or decreased vagal tone, anaesthetized mice were injected (i.p.) with either the β -adrenoceptor antagonist atenolol (2 mg/kg) or the muscarinic receptor antagonist atropine (2 mg/kg) [52] 30 minutes before Ex-4 (10 µg/kg) or saline. In contrast, atropine failed to significantly alter HR (Fig 2A), suggesting that parasympathetic activity has no contribution to chronotropic control of the heart under these experimental conditions. Atenolol decreased HR (Fig 2A), however there was no significant difference in baseline HR between Atenolol/Saline- and Atenolol/Ex-4-treated mice at the time of injections (Fig S2B). The tachycardic response to Ex-4 was abolished by systemic β -adrenoceptor blockade (Fig 2B), but not affected by pretreatment with atropine (Fig 2B), suggesting that the Ex-4-induced HR increase is due to sympathetic activation.

We subsequently confirmed those findings in freely-behaving, awake mice. Injection of 10 µg/kg Ex-4 alone induced a sustained increase in resting HR over several hours (Fig 2C,E). Pre-treatment with 2 mg/kg atenolol reduced the effect of handling stress on resting HR consistent with a decrease in sympathetic outflow to the heart (Fig 2D). Ex-4 failed to increase resting HR in conditions of systemic β -adrenoceptor blockade (Fig 2D,E).

3.3. Chemogenetic activation of PPG^{NTS} neurons

Within the brain, PPG^{NTS} neurons are the main source of endogenous GLP-1 [8]. To study their role in the modulation of HR, male Glu-Cre/GCaMP3 mice were injected with AAV8-DIO-hM3Dq:mCherry into the NTS (Fig 3A), and once hM3Dq was expressed, HR was monitored under urethane/ α -chloralose anaesthesia. Baseline HR did not differ between mice transduced to express GFP and those transduced to express hM3Dq (Fig. 3B). Activation of PPG^{NTS} neurons with CNO (2 mg/kg; i.p.) led to a significant increase in HR in hM3Dq-expressing mice, but not GFP-expressing mice (Fig 3C).

Next, we confirmed that PPG^{NTS} neuron activation is sufficient to increase HR in freely behaving mice. Male Glu-Cre mice were injected with AAV8-DIO-hM3Dq:mCherry and biotelemetry blood pressure probes were implanted. As a positive control for successful transduction, food intake was measured following CNO or saline only as previously described [8]. Injection of CNO significantly suppressed feeding in the first two hours after dark onset as compared to injection of saline only (Fig S2D).

Injection of CNO (2 mg/kg) led to a sustained increase in HR compared to injection of saline only (Fig 3D) and resulted in a shift in the distribution of resting HR values towards higher HR values (Fig 3E). This was reflected in the resting HR of hM3Dq-expressing mice, which increased significantly following injection of CNO compared to saline only (Fig 3F). Although a reduction in locomotor activity was observed in two hM3Dq-expressing mice following 2 mg/kg CNO as compared to saline, this decrease did not occur in the third hM3Dq-expressing mouse (Fig 3G).

3.4 Ex-4 elicits tachycardia when applied directly to the spinal cord

Given that a subset of PPG neurons projects to the spinal cord and form close appositions with sympathetic preganglionic neurons [37], and GLP-1R expression has been reported by *in situ* hybridisation within the spinal cord [40], we tested whether GLP-1 signalling in the cord can modulate HR. GLP-1 (0.4 μ g in 2.5 μ l saline) was applied directly to the exposed spinal cord in anaesthetized mice, which significantly increased HR as compared to application of saline alone (Fig 3H). Local application of the GLP-1R antagonist exendin(9-39) (18.75 μ g in 2.5 μ l saline) did not affect HR, indicating that there is no tonic GLP-1 activity in the spinal cord, but it strongly reduced the effect of subsequent application of GLP-1 (0.4 μ g) on HR (Fig 3I,J).

3.5. Resting HR is not affected by either acute inhibition or ablation of PPG^{NTS} neurons

Although chemogenetic activation of PPG^{NTS} neurons induced tachycardia in mice, this does not prove these neurons play a physiological role in cardiovascular control. We therefore acutely inhibited PPG^{NTS} neurons in hM4Di-expressing mice anaesthetized with urethane and α -chloralose. Male Glu-Cre/GCaMP3 mice stereotaxically injected with AAV2-DIO-hM4Di:mCherry or with AAV8-FLEX-EGFP (Fig 4A) had similar HRs prior to injection of CNO (2 mg/kg i.p.; Fig 4B), and CNO had no effect on HR (Fig 4C).

We next tested whether ablation of these cells has a significant effect on cardiovascular variables in a longitudinal study. Male Glu-Cre mice implanted with biotelemetry probes were stereotaxically injected with AAV8-mCherry-FLEX-DTA (Fig 4Di-iii, S2F; PPG^{NTS}-DTA mice) to selectively ablate PPG^{NTS} neurons as previously described [8] or AAV1/2-FLEX-Perceval as control (Fig 4E, S2G). We have demonstrated that ablation of PPG^{NTS} neurons in this manner results in an 80% reduction in GLP-1 within the spinal cord [8].

Prior to PPG^{NTS} neuron ablation, there was no difference in HR and MAP recorded over 24 hours between the two cohorts (Fig 4F). Similarly, when tested four and six weeks after PPG^{NTS} neuron ablation, no significant difference was seen between control and PPG^{NTS}-DTA mice at either timepoint (Fig 4F).

Because GLP-1R activation by Ex-4 and PPG^{NTS} chemogenetic activation were found to increase HR at times of rest, we conducted a further analysis to determine whether ablation of PPG^{NTS} neurons affected resting HR in these mice (Fig 4G). Prior to ablation, there was no difference in resting HR between control and PPG^{NTS}-DTA mice (Fig 4G). Moreover, there was little change in resting HR and MAP over time and no difference was found between control and PPG^{NTS}-DTA mice at any timepoint (Fig 4G).

To investigate whether ablation of PPG^{NTS} neurons affects HR and MAP whilst ambulatory, biotelemetry data were extracted specifically during periods of activity. As expected, HR during activity was higher than resting HR (Fig 4Hi 'control baseline' and Fig 4Hi 'control baseline', respectively $p < 0.0001$, Student's paired t-test). HR during activity remained similar from baseline to six weeks and there was no difference between control and PPG^{NTS}-DTA mice six weeks after surgery (Fig 4Hi). Similarly, there was no effect of ablation of PPG^{NTS} neurons on active MAP during activity (Fig 4Hii).

We next assessed the effects of PPG^{NTS} neuron ablation on locomotor activity. Fig 5A shows plots of activity over 24 hours from representative control and PPG^{NTS}-DTA mice before and six weeks after surgery. Ablation of PPG^{NTS} neurons did not affect activity levels and six

weeks post-surgery there was no difference in the time that control and PPG^{NTS}-DTA mice spent inactive during light phase (Fig 5B) or dark phase (Fig 5C), suggesting that loss of PPG^{NTS} neurons does not affect locomotor activity.

Taken together these data suggest that PPG^{NTS} neurons are not necessary for modulation of HR or ABP under resting conditions. They also do not influence locomotor activity levels.

3.6 Ex-4-induced tachycardia is independent of PPG^{NTS} neuron activity

To investigate whether systemic injection of Ex-4 requires PPG neurons for its full effect on HR, we injected freely-behaving control and PPG^{NTS}-DTA mice with 10 µg/kg Ex-4 i.p. nine weeks post-surgery.

As seen previously, i.p. injection with 10 µg/kg Ex-4 led to an increase in HR (Fig 6A). The response was similar in control and PPG^{NTS} ablated animals (Fig 6A) and there was no difference in the change in resting HR in response to both saline and 10 µg/kg Ex-4 between control and PPG^{NTS}-DTA mice (Fig 6B, S2E). In support of these findings, i.p. injection of Ex-4 (10 µg/kg), failed to elicit cFos expression in PPG neurons (Fig. 6C), whilst increasing cFos in the area postrema (Fig S2H,I), suggesting PPG neurons are not necessary for effects of systemic Ex-4 on HR in mice.

4. Discussion

In this study we demonstrate for the first time that activation of PPG^{NTS} neurons induces robust increases in HR. We also confirm previous reports that systemic administration of GLP-1RAs increases HR via stimulation of sympathoexcitatory mechanisms in mice [1]. We demonstrate that GLP-1R activation in the spinal cord is sufficient to elicit tachycardic responses and we also found that PPG^{NTS} neurons are capable of increasing resting HR, but not ABP. Interestingly, we failed to observe a tonic drive of PPG^{NTS} neurons on HR in either anaesthetized or freely behaving mice. Our findings provide evidence that PPG^{NTS} neurons have the capacity to affect central cardiovascular control and sympathetic activity but suggest they do not provide a tonic input to cardiac chronotropic function.

This study was performed primarily on mixed sex cohorts, although the telemetry cohorts were made up of male mice only. The study did not reveal any sex differences in any parameters tested, but was also not specifically designed nor powered for that purpose.

4.1 Mechanisms underlying GLP-1R-mediated tachycardia

Although the tachycardic effects of GLP-1R stimulation have proven robust and reproducible, particularly in rodents, the underlying neurocircuits remain unclear. GLP-1R-mediated cardiovascular effects may involve a combination of peripheral and central pathways involving GLP-1Rs both in the brain and on the heart [1, 3, 22, 50, 53]. Furthermore, both the parasympathetic [2, 3, 5, 25] and sympathetic nervous system [1, 13, 24, 29] have been implicated in the tachycardic response to GLP-1R stimulation.

The most commonly proposed scenario for GLP-1R-mediated tachycardia involves both peripheral and central mechanisms [1, 3, 24]. GLP-1Rs are found in subsets of cardiac myocytes, cardiac blood vessels, as well as the sinoatrial node, of mice and humans [39, 54, 55], and mice lacking cardiac GLP-1Rs have reduced HR responses to the GLP-1R agonist, liraglutide [1]. However, no direct effect of GLP-1R agonism on isolated hearts has been found [1, 50], leaving the role of cardiac GLP-1R-mediated tachycardia elusive.

Findings presented here support a role for the sympathetic nervous system in mediating Ex-4-induced tachycardia. I.p. Ex-4 failed to increase HR in the absence of sympathetic input to the heart in both anaesthetized and freely behaving mice. Moreover, the tachycardic response to i.p. Ex-4 persists in the presence of the muscarinic acetylcholine receptor antagonist atropine, demonstrating that parasympathetic input is not necessary for cardiovascular effects of systemic GLP-1R stimulation. These findings correspond with earlier reports that GLP-1R stimulation activates sympathetic preganglionic neurons [24, 29] and that propranolol, a non-selective β -blocker, abolishes the tachycardic response to liraglutide in mice [1].

4.2 Peripheral and central contributions to GLP-1R-mediated tachycardia

Cardiac sympathetic nervous activity is initiated within the central nervous system, involving presympathetic neurons in hypothalamus and brainstem, which in turn innervate sympathetic preganglionic neurons in the thoracic spinal cord. These project to the postganglionic neurons located in the ganglia of the paravertebral chain, which innervate the sinoatrial node as well as the ventricles of the heart. GLP-1Rs are potentially present at all levels. Consequently, Ex-4-induced tachycardia could arise from all these levels, whilst PPG neurons only innervate presympathetic areas of hypothalamus and brainstem, as well as preganglionic sympathetic neurons in the IML and CAA of the spinal cord [36, 37]. Here we demonstrate that direct

application of Ex-4 to the thoracic spinal cord elicits tachycardia, supporting the notion that activation of spinal GLP-1R is sufficient to drive increases in HR [37, 40].

Whilst Ex-4 increased HR in both anaesthetized and conscious mice, GLP-1 only produced obvious tachycardia in anaesthetized mice. This is most likely because conscious mice show a strong stress response to handling and i.p. injection, and HR only returns to resting levels more than 30 min after the injection. Presumably, GLP-1 is inactivated by that time so that no lasting response is recorded [4, 24, 56, 57]. In contrast, in anaesthetized mice Ex-4 and GLP-1 produced responses of similar magnitude, suggesting that both substances reach the relevant receptors with similar efficiency.

4.3. GLP-1R effects on blood pressure

While we found clear effects of GLP-1R stimulation of HR, freely behaving mice showed no change in ABP in response to 10 µg/kg Ex-4. In accordance, one study found no effect of liraglutide on systolic and diastolic blood pressure in mice, although the same study reported antihypertensive effects of liraglutide in mice with pharmacologically elevated ABP (Kim et al 2013). Some studies have reported robust hypertensive effects of GLP-1 analogues in rats [24, 25], whereas others found little evidence for an effect on ABP [27], suggesting there could be relevant species differences or that differences in experimental conditions affect ABP responses to GLP-1R stimulation.

4.4 PPG^{NTS} neurons have the ability to induce tachycardia

We demonstrate here that chemogenetic activation of PPG^{NTS} neurons increases HR. Activation of PPG neurons is expected to lead to release of GLP-1 and glutamate [58, 59] in CNS areas involved in cardiovascular control, such as the PVN, arcuate nucleus, RVLM, CAA, and IML [38, 40, 60]. The dense innervation of the spinal cord IML/CAA by PPG neurons [37] and the robust effects of direct application of Ex-4 to the thoracic spinal cord reported here, strongly implicate PPG^{NTS→IML/CAA} projections in PPG-mediated tachycardia. Selective viral targeting of these projections in future studies are thus warranted to interrogate their specific role in the modulation of cardiovascular function by GLP-1.

Interestingly, we found that the tachycardic effects of both Ex-4 and PPG^{NTS} neuron activation were mainly on resting HR. This may reflect a ceiling effect, whereby GLP-1R-mediated activation of the sympathetic nervous system has no additional effect on HR at

times of increased ambulatory activity and/or stress. In support of this, under urethane anaesthesia, which is known to increase sympathetic outflow, Ex-4-induced tachycardia was attenuated. These data also suggest that common mechanisms underlie the cardiovascular effects of PPG^{NTS} activation and GLP-1R stimulation. Importantly, we cannot rule out that the relatively large dose of Ex-4 used in this study (10 µg/kg) may lead to higher levels of GLP-1R engagement than chemogenetic activation of PPG^{NTS} neurons, and additionally, Ex-4 would potentially reach GLP-1Rs on cells that are not innervated by PPG neurons, such as postganglionic sympathetic neurons or cardiac myocytes, and thus replicating the effects of gut-derived GLP-1.

4.5 Endogenous, central GLP-1 in cardiovascular control

Whilst exogenous GLP-1 and its analogues are clearly capable of eliciting a tachycardic response, it is less clear whether endogenous GLP-1 released from either the brain or the gut plays a role in day-to-day HR regulation. This question has been addressed in two ways. Firstly, Barragan et al. infused the GLP-1R antagonist, Ex-9 either i.v. or intracerebroventricular and found no effect on HR and ABP [3, 4]. As an alternative approach we inhibited or ablated the PPG^{NTS} neurons and thereby the native source of GLP-1 within the CNS [8]. In support of the results obtained with Ex-9, the current study revealed no effect of the loss of PPG^{NTS} neuron activity on HR or ABP under typical physiological conditions. Our findings corroborate previous reports that HR is unaffected by both genetic disruption of GLP-1R [53] as well as lack of hypothalamic GLP-1R [13].

4.6 Relationship between exogenous GLP-1R agonists and PPG neurons

Here we have shown that both activation of PPG^{NTS} neurons and systemic application of Ex-4 increase HR via stimulation of the sympathetic nervous system. We have also shown that peripherally-administered Ex-4 does not activate PPG neurons. This suggests that either PPG^{NTS} neurons and Ex-4 both have access to the same neuronal GLP-1R population(s) or that they activate sympathetic inputs to the heart via different pathways. The action of PPG^{NTS} neurons is limited to receptors within areas of the CNS, which receive input from PPG neurons [35-38]. On the other hand, systemic Ex-4 may reach GLP-1R in both the periphery and in the CNS, although it is becoming increasingly evident that GLP-1RAs and antagonists may not readily cross the blood brain barrier to access all CNS GLP-1R populations [61-63]. In fact, assuming that access to the CNS is similar for peripherally

administered Ex-4 as it is for fluorescently labelled liraglutide [62, 63], we would expect that Ex-4 acts in either PVN, AP/NTS or on spinal preganglionic sympathetic neurons to affect HR. This is supported by a previous finding that peripheral Ex-4 leads to robust activation of tyrosine hydroxylase-containing cells within the AP [29].

4.7 GLP-1 and stress

Inhibition of PPG^{NTS} neurons did not reduce HR in anaesthetized mice, indicating that there is no tonic effect of PPG^{NTS} neurons on sympathetic outflow to the heart under these conditions. We have recently shown that PPG^{NTS} neurons are not involved in the day-to-day regulation of food intake, but are recruited to terminate unusually large meals, and mediate stress-induced hypophagia [8, 9]. Assuming that this hypophagic effects of PPG^{NTS} neurons comprises part of a wider GLP-1-mediated physiological response to acute stress [10, 12], it is plausible that the tachycardic action of PPG^{NTS} neurons also specifically occurs under conditions of stress [10]. When an animal meets a stressor, rises in HR and blood pressure are induced in order to provide enough oxygen, in preparation for the fight and flight response [64, 65]. Therefore, the tachycardia induced by activation of the PPG^{NTS} neurons could represent the role of the PPG neurons during a stress response and would explain why inhibition of the neurons does not reduce HR under resting conditions. In support of this, Ghosal et al (2017) demonstrated that hypothalamic GLP-1Rs contribute to stress-induced tachycardia [13] and the recent whole-brain mapping of monosynaptic inputs to PPG^{NTS} neurons revealed dense innervation from stress-responsive brain regions involved in autonomic control [66]. Future investigations should focus on the necessity for PPG neuron activity, and in particular the PPG^{NTS}→CAA/IML pathway, in the cardiovascular and hypophagic responses to stress.

Conclusion

In this study, we confirm the sympathoexcitatory effects of GLP-1R stimulation and show for the first time that direct application of GLP-1 to the spinal cord is sufficient to elicit tachycardic responses. We also demonstrate that, while GLP-1-producing PPG^{NTS} neurons do not provide a tonic sympathetic drive to the heart and are not necessary for the tachycardic effects of systemic Ex-4, they do have the ability to increase HR in mice. This suggests that under certain physiological conditions, PPG neurons may lead to sympathoexcitation, potentially by triggering release of GLP-1 in the spinal cord, resulting in an increase in

chronotropic sympathetic drive to the heart. These physiological conditions are likely to include stress, which is known to increase sympathetic nervous system activity and have been shown to activate PPG neurons [8, 9, 21]. Our findings reveal a potential novel role for GLP-1 and PPG neurons in cardiovascular control through activation of spinal cord neurons.

Acknowledgements

This study was supported by MRC project grant MR/N02589X/1 to ST, a British Heart Foundation grant FS/14/43/ 30960 (PhD Studentship DRC) to ST, and a UCL Graduate Research Scholarship to MKH. AVG is a Wellcome Trust Senior Research Fellow (Ref: 200893). We would also like to thank Richard Ang for invaluable technical advice and training.

Author contributions

The project was conceived by ST and AVG. Data generation was led by MKH, NM and DRC with the assistance of DIB, JER and ST. FR provided mouse lines. The manuscript was drafted by MKH and ST with input from all other authors.

References

1. Baggio, L.L., et al., *The autonomic nervous system and cardiac GLP-1 receptors control heart rate in mice*. *Mol Metab*, 2017. **6**(11): p. 1339-1349.
2. Cabou, C., et al., *Brain glucagon-like peptide-1 regulates arterial blood flow, heart rate, and insulin sensitivity*. *Diabetes*, 2008. **57**(10): p. 2577-87.
3. Barragan, J.M., et al., *Neural contribution to the effect of glucagon-like peptide-1-(7-36) amide on arterial blood pressure in rats*. *Am J Physiol*, 1999. **277**(5): p. E784-91.
4. Barragan, J.M., et al., *Interactions of exendin-(9-39) with the effects of glucagon-like peptide-1-(7-36) amide and of exendin-4 on arterial blood pressure and heart rate in rats*. *Regul Pept*, 1996. **67**(1): p. 63-8.
5. Griffioen, K.J., et al., *GLP-1 receptor stimulation depresses heart rate variability and inhibits neurotransmission to cardiac vagal neurons*. *Cardiovasc Res*, 2011. **89**(1): p. 72-8.
6. Robinson, L.E., et al., *Effects of exenatide and liraglutide on heart rate, blood pressure and body weight: systematic review and meta-analysis*. *BMJ Open*, 2013. **3**(1).
7. Nakatani, Y., et al., *Effects of GLP-1 Receptor Agonists on Heart Rate and the Autonomic Nervous System Using Holter Electrocardiography and Power Spectrum Analysis of Heart Rate Variability*. *Diabetes Care*, 2016. **39**(2): p. e22-3.
8. Holt, M.K., et al., *Preproglucagon Neurons in the Nucleus of the Solitary Tract Are the Main Source of Brain GLP-1, Mediate Stress-Induced Hypophagia, and Limit Unusually Large Intakes of Food*. *Diabetes*, 2019. **68**(1): p. 21-33.
9. Terrill, S.J., et al., *Endogenous GLP-1 in lateral septum promotes satiety and suppresses motivation for food in mice*. *Physiol Behav*, 2019. **206**: p. 191-199.

10. Holt, M.K. and S. Trapp, *The physiological role of the brain GLP-1 system in stress*. Cogent Biol, 2016. **2**(1): p. 1229086.
11. Maniscalco, J.W., et al., *Negative Energy Balance Blocks Neural and Behavioral Responses to Acute Stress by "Silencing" Central Glucagon-Like Peptide 1 Signaling in Rats*. J Neurosci, 2015. **35**(30): p. 10701-14.
12. Ghosal, S., B. Myers, and J.P. Herman, *Role of central glucagon-like peptide-1 in stress regulation*. Physiol Behav, 2013. **122**: p. 201-7.
13. Ghosal, S., et al., *Disruption of Glucagon-Like Peptide 1 Signaling in Sim1 Neurons Reduces Physiological and Behavioral Reactivity to Acute and Chronic Stress*. Journal of Neuroscience, 2017. **37**(1): p. 184-193.
14. Turton, M.D., et al., *A role for glucagon-like peptide-1 in the central regulation of feeding*. Nature, 1996. **379**(6560): p. 69-72.
15. Tang-Christensen, M., et al., *Central administration of GLP-1-(7-36) amide inhibits food and water intake in rats*. Am J Physiol, 1996. **271**(4 Pt 2): p. R848-56.
16. Gaykema, R.P., et al., *Activation of murine pre-proglucagon-producing neurons reduces food intake and body weight*. J Clin Invest, 2017. **127**: p. 1031-1045.
17. Ulrich-Lai, Y.M., et al., *Stress exposure, food intake and emotional state*. Stress, 2015. **18**(4): p. 381-99.
18. Myers, B., et al., *Ascending mechanisms of stress integration: Implications for brainstem regulation of neuroendocrine and behavioral stress responses*. Neurosci Biobehav Rev, 2017. **74**(Pt B): p. 366-375.
19. Herman, J.P., et al., *Regulation of the Hypothalamic-Pituitary-Adrenocortical Stress Response*. Compr Physiol, 2016. **6**(2): p. 603-21.
20. Zheng, H., et al., *Chronic Suppression of Glucagon-Like Peptide-1 Receptor (GLP1R) mRNA Translation in the Rat Bed Nucleus of the Stria Terminalis Reduces Anxiety-Like Behavior and Stress-Induced Hypophagia, But Prolongs Stress-Induced Elevation of Plasma Corticosterone*. J Neurosci, 2019. **39**(14): p. 2649-2663.
21. Maniscalco, J.W., A.D. Kreisler, and L. Rinaman, *Satiation and stress-induced hypophagia: examining the role of hindbrain neurons expressing prolactin-releasing Peptide or glucagon-like Peptide 1*. Front Neurosci, 2012. **6**: p. 199.
22. Hayes, M.R., K.P. Skibicka, and H.J. Grill, *Caudal brainstem processing is sufficient for behavioral, sympathetic, and parasympathetic responses driven by peripheral and hindbrain glucagon-like-peptide-1 receptor stimulation*. Endocrinology, 2008. **149**(8): p. 4059-68.
23. Vrang, N. and P.J. Larsen, *Preproglucagon derived peptides GLP-1, GLP-2 and oxyntomodulin in the CNS: role of peripherally secreted and centrally produced peptides*. Prog Neurobiol, 2010. **92**(3): p. 442-62.
24. Yamamoto, H., et al., *Glucagon-like peptide-1 receptor stimulation increases blood pressure and heart rate and activates autonomic regulatory neurons*. J Clin Invest, 2002. **110**(1): p. 43-52.
25. Barragan, J.M., R.E. Rodriguez, and E. Blazquez, *Changes in arterial blood pressure and heart rate induced by glucagon-like peptide-1-(7-36) amide in rats*. Am J Physiol, 1994. **266**(3 Pt 1): p. E459-66.
26. Kang, Y.M. and C.H. Jung, *Cardiovascular Effects of Glucagon-Like Peptide-1 Receptor Agonists*. Endocrinol Metab (Seoul), 2016. **31**(2): p. 258-74.
27. Edwards, C.M., A.V. Edwards, and S.R. Bloom, *Cardiovascular and pancreatic endocrine responses to glucagon-like peptide-1(7-36) amide in the conscious calf*. Exp Physiol, 1997. **82**(4): p. 709-16.
28. Edwards, C.M., et al., *Subcutaneous glucagon-like peptide-1 (7-36) amide is insulinotropic and can cause hypoglycaemia in fasted healthy subjects*. Clin Sci (Lond), 1998. **95**(6): p. 719-24.

29. Yamamoto, H., et al., *Glucagon-like peptide-1-responsive catecholamine neurons in the area postrema link peripheral glucagon-like peptide-1 with central autonomic control sites*. J Neurosci, 2003. **23**(7): p. 2939-46.
30. Terrill, S.J., C.B. Maske, and D.L. Williams, *Endogenous GLP-1 in lateral septum contributes to stress-induced hypophagia*. Physiol Behav, 2018. **192**: p. 17-22.
31. Kinzig, K.P., et al., *CNS glucagon-like peptide-1 receptors mediate endocrine and anxiety responses to interoceptive and psychogenic stressors*. J Neurosci, 2003. **23**(15): p. 6163-70.
32. Tauchi, M., et al., *Role of central glucagon-like peptide-1 in hypothalamo-pituitary-adrenocortical facilitation following chronic stress*. Exp Neurol, 2008. **210**(2): p. 458-66.
33. Zhang, R., et al., *Glucocorticoid regulation of preproglucagon transcription and RNA stability during stress*. Proc Natl Acad Sci U S A, 2009. **106**(14): p. 5913-8.
34. Gil-Lozano, M., et al., *GLP-1(7-36)-amide and Exendin-4 stimulate the HPA axis in rodents and humans*. Endocrinology, 2010. **151**(6): p. 2629-40.
35. Llewellyn-Smith, I.J., et al., *Preproglucagon (PPG) neurons innervate neurochemically identified autonomic neurons in the mouse brainstem*. Neuroscience, 2013. **229**: p. 130-43.
36. Llewellyn-Smith, I.J., et al., *Preproglucagon neurons project widely to autonomic control areas in the mouse brain*. Neuroscience, 2011. **180**: p. 111-21.
37. Llewellyn-Smith, I.J., et al., *Spinally projecting preproglucagon axons preferentially innervate sympathetic preganglionic neurons*. Neuroscience, 2015. **284**: p. 872-87.
38. Cork, S.C., et al., *Distribution and Characterisation of Glucagon-Like Peptide-1 receptor expressing cells in the mouse brain*. Molecular Metabolism, 2015. **4**: p. 718-731.
39. Richards, P., et al., *Identification and characterization of GLP-1 receptor-expressing cells using a new transgenic mouse model*. Diabetes, 2014. **63**(4): p. 1224-33.
40. Merchenthaler, I., M. Lane, and P. Shughrue, *Distribution of pre-pro-glucagon and glucagon-like peptide-1 receptor messenger RNAs in the rat central nervous system*. J Comp Neurol, 1999. **403**(2): p. 261-80.
41. Parker, H.E., et al., *Predominant role of active versus facilitative glucose transport for glucagon-like peptide-1 secretion*. Diabetologia, 2012. **55**(9): p. 2445-55.
42. Holt, M.K., et al., *Serotonergic modulation of the activity of GLP-1 producing neurons in the nucleus of the solitary tract in mouse*. Mol Metab, 2017. **6**(8): p. 909-921.
43. Anesten, F., et al., *Preproglucagon neurons in the hindbrain have IL-6 receptor-alpha and show Ca²⁺ influx in response to IL-6*. Am J Physiol Regul Integr Comp Physiol, 2016. **311**(1): p. R115-23.
44. Reimann, F., et al., *Glucose sensing in L cells: a primary cell study*. Cell Metab, 2008. **8**(6): p. 532-9.
45. Barrera, J.G., et al., *Differences in the central anorectic effects of glucagon-like peptide-1 and exendin-4 in rats*. Diabetes, 2009. **58**(12): p. 2820-7.
46. Mack, C.M., et al., *Antiobesity action of peripheral exenatide (exendin-4) in rodents: effects on food intake, body weight, metabolic status and side-effect measures*. Int J Obes (Lond), 2006. **30**(9): p. 1332-40.
47. Williams, D.L., D.G. Baskin, and M.W. Schwartz, *Evidence that intestinal glucagon-like peptide-1 plays a physiological role in satiety*. Endocrinology, 2009. **150**(4): p. 1680-7.
48. Kanoski, S.E., et al., *Peripheral and central GLP-1 receptor populations mediate the anorectic effects of peripherally administered GLP-1 receptor agonists, liraglutide and exendin-4*. Endocrinology, 2011. **152**(8): p. 3103-12.
49. Dickson, S.L., et al., *The glucagon-like peptide 1 (GLP-1) analogue, exendin-4, decreases the rewarding value of food: a new role for mesolimbic GLP-1 receptors*. J Neurosci, 2012. **32**(14): p. 4812-20.
50. Ang, R., et al., *Modulation of Cardiac Ventricular Excitability by GLP-1 (Glucagon-Like Peptide-1)*. Circ Arrhythm Electrophysiol, 2018. **11**(10): p. e006740.

51. Shimokawa, A., et al., *Differential effects of anesthetics on sympathetic nerve activity and arterial baroreceptor reflex in chronically instrumented rats*. J Auton Nerv Syst, 1998. **72**(1): p. 46-54.
52. Iwasaki, K.I., et al., *Parasympathetic nervous activity after administration of atropine and neostigmine using heart rate spectral analysis*. J Anesth, 1997. **11**(1): p. 22-26.
53. Gros, R., et al., *Cardiac function in mice lacking the glucagon-like peptide-1 receptor*. Endocrinology, 2003. **144**(6): p. 2242-52.
54. Kim, M., et al., *GLP-1 receptor activation and Epac2 link atrial natriuretic peptide secretion to control of blood pressure*. Nat Med, 2013. **19**(5): p. 567-75.
55. Baggio, L.L., et al., *GLP-1 Receptor Expression Within the Human Heart*. Endocrinology, 2018. **159**(4): p. 1570-1584.
56. Holst, J.J., *The physiology of glucagon-like peptide 1*. Physiol Rev, 2007. **87**(4): p. 1409-39.
57. Orskov, C., A. Wettergren, and J.J. Holst, *Biological effects and metabolic rates of glucagonlike peptide-1 7-36 amide and glucagonlike peptide-1 7-37 in healthy subjects are indistinguishable*. Diabetes, 1993. **42**(5): p. 658-61.
58. Zheng, H., et al., *Glutamatergic phenotype of glucagon-like peptide 1 neurons in the caudal nucleus of the solitary tract in rats*. Brain Struct Funct, 2014.
59. Trapp, S. and S.C. Cork, *PPG neurons of the lower brain stem and their role in brain GLP-1 receptor activation*. Am J Physiol Regul Integr Comp Physiol, 2015. **309**(8): p. R795-804.
60. Alvarez, E., et al., *Expression of the glucagon-like peptide-1 receptor gene in rat brain*. J Neurochem, 1996. **66**(3): p. 920-7.
61. Ast, J., et al., *Super-resolution microscopy compatible fluorescent probes reveal endogenous glucagon-like peptide-1 receptor distribution and dynamics*. Nat Commun, 2020. **11**(1): p. 467.
62. Salinas, C.B.G., et al., *Integrated Brain Atlas for Unbiased Mapping of Nervous System Effects Following Liraglutide Treatment*. Sci Rep, 2018. **8**(1): p. 10310.
63. Secher, A., et al., *The arcuate nucleus mediates GLP-1 receptor agonist liraglutide-dependent weight loss*. J Clin Invest, 2014. **124**(10): p. 4473-88.
64. Myers, B., *Corticolimbic regulation of cardiovascular responses to stress*. Physiol Behav, 2017. **172**: p. 49-59.
65. Obrist, P.A., et al., *Sympathetic influences on cardiac rate and contractility during acute stress in humans*. Psychophysiology, 1974. **11**(4): p. 405-27.
66. Holt, M.K., et al., *Synaptic Inputs to the Mouse Dorsal Vagal Complex and Its Resident Preproglucagon Neurons*. J Neurosci, 2019. **39**(49): p. 9767-9781.
67. Krashes, M.J., et al., *Rapid, reversible activation of AgRP neurons drives feeding behavior in mice*. J Clin Invest, 2011. **121**(4): p. 1424-8.
68. Murray, A.J., et al., *Parvalbumin-positive CA1 interneurons are required for spatial working but not for reference memory*. Nat Neurosci, 2011. **14**(3): p. 297-9.
69. Tarasov, A.I., et al., *The mitochondrial Ca²⁺ uniporter MCU is essential for glucose-induced ATP increases in pancreatic beta-cells*. PLoS One, 2012. **7**(7): p. e39722.

Table 1. Sources of virus and antibody preparations used.

Virus/Antibody	Application	Source	References
AAV8-DIO-hM ₃ Dq:mCherry	Activation of Cre-expressing PPG neurons	VVF, ZNZ, Zurich	pAAV-hSyn-DIO-hM3D(Gq)-mCherry was a gift from Bryan Roth [67]

AAV8-mCherry-FLEX-DTA	Ablation of Cre-expressing PPG neurons	UNC Vectorcore	pAAV-mCherry-flex-dtA was a gift from Naoshige Uchida.
AAV2-DIO-hM ₄ Di:mCherry	Inhibition of Cre-expressing PPG neurons	VVF, ZNZ, Zurich	pAAV-hSyn-DIO-hM4D(Gi)-mCherry was a gift from Bryan Roth [67]
AAV1/2-FLEX-Perceval	Control for viral transduction	Made in house.	pAAV-FLEX-empty was a gift from Bill Wisden [68] pShuttleCMV-Perceval was a gift from Guy Rutter [69]
AAV8-DIO-EGFP	Control for viral transduction	VVF, ZNZ, Zurich	pAAV-hSyn-DIO-EGFP was a gift from Bryan Roth
Chicken anti-GFP; Alexa488 goat anti-chicken; 1:1000	GCaMP3, EGFP, YFP, Perceval	Abcam AB13970; Invitrogen #A-11039	[42]
Rabbit anti-dsRed; Cy3 sheep anti-rabbit; 1:1000	mCherry, tdRFP	Takara Bio #632496; Sigma #C2306	[38]
Rabbit anti-cFOS 1:500; Cy3 sheep anti-rabbit 1:1000	cFOS	Merck #ABE457; Sigma #C2306	

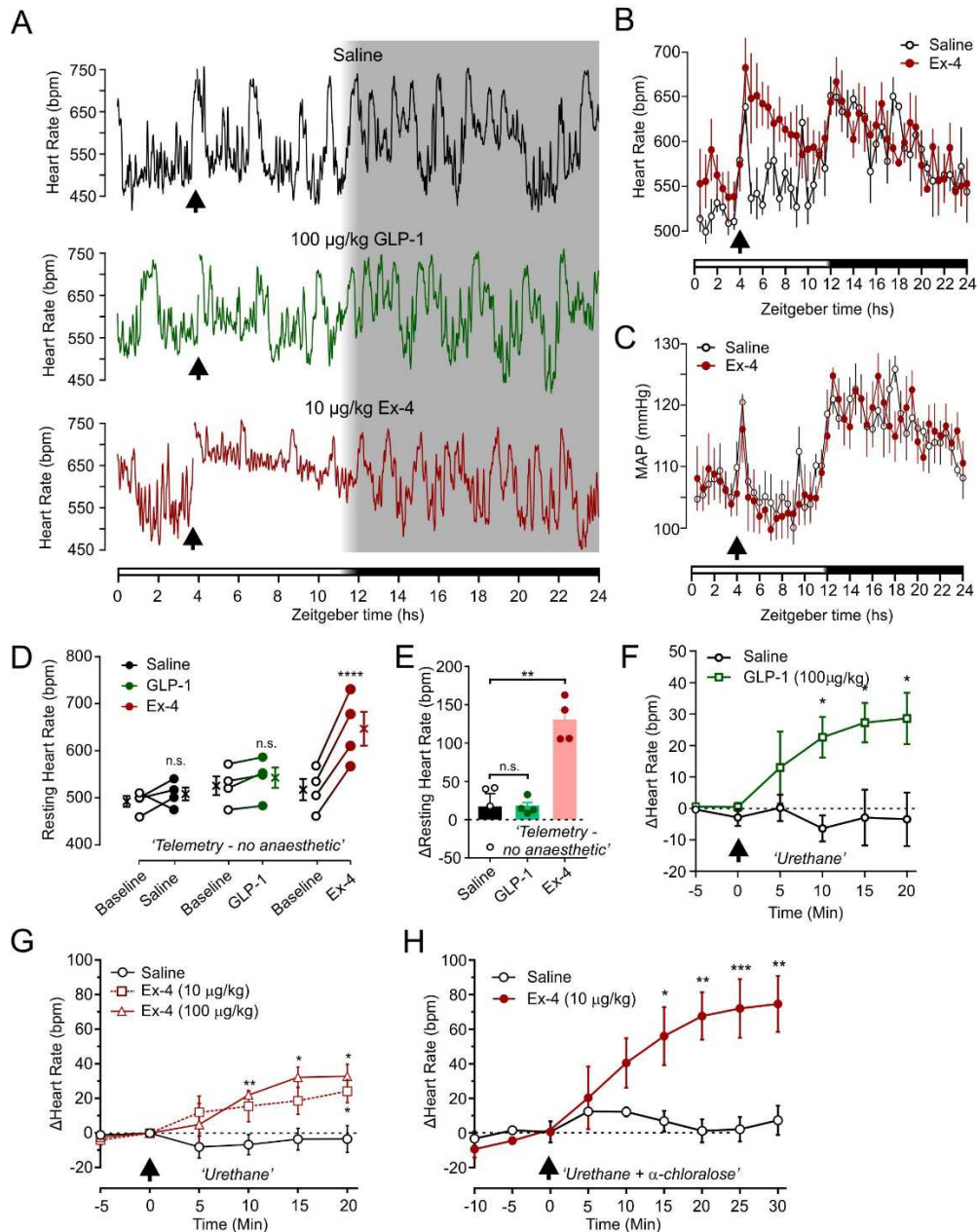


Figure 1: Systemic activation of GLP-1Rs induces tachycardia without affecting ABP

A) Representative HR recording from a conscious, freely-moving mouse injected i.p. with either saline (black, top), 100 µg/kg GLP-1(7-36) (GLP-1, green, middle), or 10 µg/kg Ex-4 (red, bottom) recorded over 24 hours as indicated by zeitgeber time at the bottom. Arrows indicate times of injection and the bar at the bottom indicates light (white bar) and dark (black bar) phases with a brief period of half-light indicated by a white to black gradient. Traces are running averages over 200 s. B) HR and C) MAP of mice (n=4) injected i.p. with saline (black) and 10 µg/kg Ex-4 (red) four hours into light phase (arrow). Shown here are mean±SEM of four mice taken every 30 mins over 24 hours as indicated by Zeitgeber time. Bars at the bottom indicate light (white bar) and dark (black bar) phases with a brief period of half-light indicated by a white to black gradient. D) Mice implanted with biotelemetry probes were injected i.p. with saline (black), 100 µg/kg GLP-1 (green), and 10 µg/kg Ex-4 (red) four hours into light phase. Resting HRs of individual mice were determined before (hours 2-3) and after (hours 5-6) i.p. injections. Paired data from individual mice are plotted as well as mean±SEM values (n=4). Drug x time: $F_{(1, 3)} = 22.35$, $p=0.018$. **** $p<0.0001$, n.s.: not

significant, Sidak's matched pairs multiple comparisons test. E) Change in resting HR from baseline determined from D) following injections of saline (black), GLP-1 (green), and Ex-4 (red). Data from individual mice are shown as well as mean \pm SEM for each treatment (n=4). **p<0.01, n.s.: not significant, Dunnett's multiple comparisons test. F) Change in HR from baseline in urethane-anaesthetized mice injected i.v. at timepoint 0 (arrow) with either saline (n=5) or GLP-1 (100 μ g/kg, n=5), Two-way mixed-model ANOVA: Drug x time $F_{(5, 40)} = 4.824$, p=0.0015, followed by post-hoc Dunnett's test (*p<0.05). G) Change in HR from baseline in urethane-anaesthetized mice injected i.p. with either saline (n=3) Ex-4 (10 μ g/kg, n=3) or Ex-4 (100 μ g/kg, n=3) at timepoint 0 (arrow). Two-way mixed model ANOVA: Drug x time $F_{(8, 28)} = 2.53$, p=0.0329, followed by post-hoc Dunnett's test (*p<0.05, **p<0.01 vs saline). H) Change in HR from baseline in urethane/ α -chloralose-anaesthetized mice injected i.p. with either saline (n=3) or Ex-4 (10 μ g/kg, n=3) at timepoint 0 (arrow). Two-way mixed-model ANOVA: Drug x time $F_{(6, 36)} = 7.459$, p<0.0001, followed by Sidak's multiple comparisons test (*p<0.05, **p<0.01, ***p<0.001).

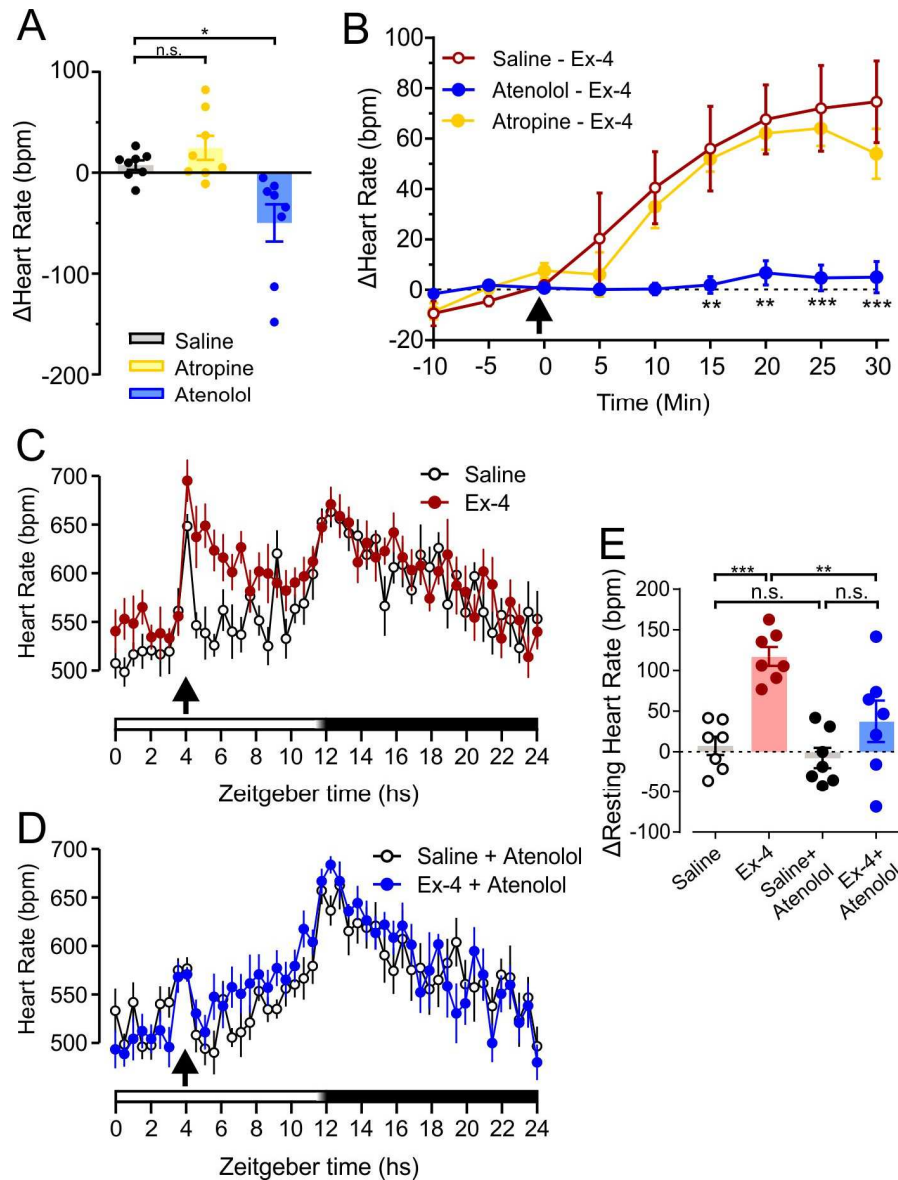


Figure 2: Systemic GLP-1R activation induces tachycardia via the sympathetic nervous system in anaesthetized and freely behaving mice

A) Change in HR in urethane/ α -chloralose-anaesthetized mice 25 min after i.p. injection of saline (n=8), atropine (2 mg/kg, n=8) or atenolol (2 mg/kg, n=8). One-way ANOVA $F_{(2,21)} = 8,808$, $p=0.0017$, followed by post-hoc Dunnett's test (* $p<0.05$) B) Change in HR from baseline in anaesthetized mice following i.p. injection of Ex-4 (10 μ g/kg; arrow) in the absence (n=4, Sal-Ex-4) or presence (n=4, Aten-Ex-4) of atenolol (2 mg/kg, i.p.) injected 30 mins earlier. Two-way mixed model ANOVA: drug x time $F_{(12, 54)} = 3.562$, $p=0.0006$, followed by post-hoc Dunnett's test (** $p<0.01$, *** $p<0.001$ vs Sal-Ex4). C, D) Mice implanted with biotelemetry probes (n=7) were injected i.p. with saline or Ex-4 (10 μ g/kg, arrow) four hours into light phase in the absence (C) or presence (D) of atenolol (2 mg/kg) injected 15 mins earlier. Shown here are mean \pm SEM taken every 30 mins over 24 hours as indicated by zeitgeber time on the x-axis. Arrows indicate time of injection and the bars at the bottom indicate light (white bar) and dark (black bar) phases with a period of half-light indicated by a white to black gradient. E) Change in HR (1-2 hours post-injection) from baseline (1-2 hours before injection) in biotelemetry probe-implanted mice in response to saline or Ex-4 (10 μ g/kg) in the absence or presence of atenolol (2 mg/kg, n=7). Pre-

treatment x drug: $F_{(1, 6)} = 13.84$, $p=0.0099$, ** $p>0.01$, *** $p<0.001$ and n.s.: not significant, Sidak's multiple comparisons test.

Journal Pre-proof

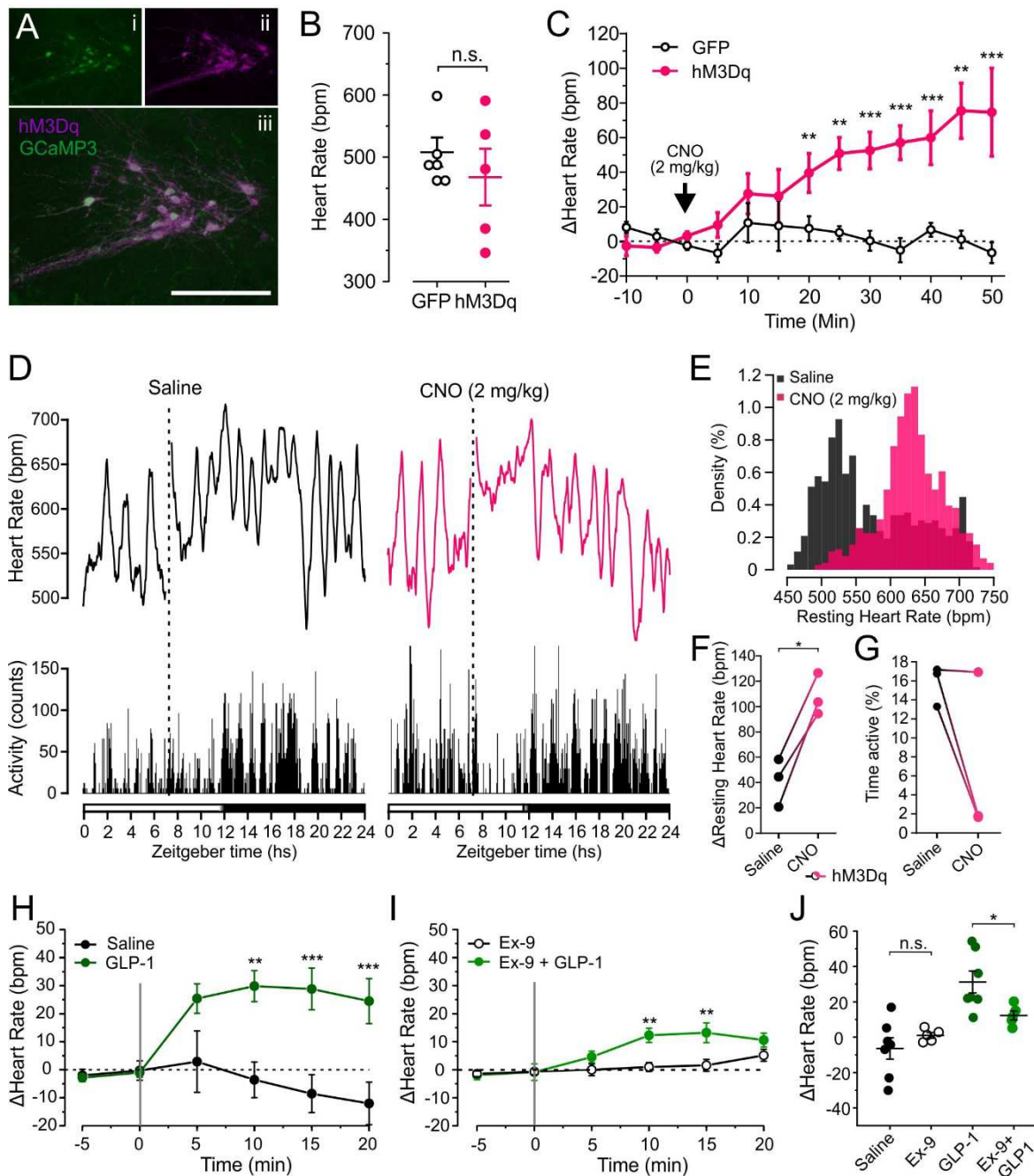


Figure 3: Chemogenetic activation of PPG^{NTS} neurons and direct application of GLP-1 to the spinal cord increases HR in mice

A) Representative images of immunofluorescence double-labeling of GCaMP3 (green, indicating PPG^{NTS} neurons) and hM3Dq:mCherry (magenta) in the caudal NTS. Scale bar: 200 μ m B) Baseline HR prior to injection of CNO from urethane/ α -chloralose-anaesthetized mice expressing either GFP or hM3Dq in PPG^{NTS} neurons (unpaired t-test). C) Change in HR from baseline in response to CNO (2 mg/kg) injected after 10 mins baseline recording (arrow) from urethane/ α -chloralose-anaesthetized mice expressing either GFP or hM3Dq in PPG^{NTS} neurons. Two-way ANOVA: Virus x time $F_{(9, 72)} = 5.477$, $p < 0.0001$; followed by Sidak's multiple comparisons test (** $p < 0.01$, *** $p < 0.001$). D) Representative 24 hour HR (top) and locomotor activity (bottom) recording of a freely behaving mouse expressing hM3Dq in PPG^{NTS} neurons injected i.p. with either saline (left) or 2 mg/kg CNO (right). Dotted lines indicate times of injection and the bar at the bottom indicates light (white bar)

and dark (black bar) phases with a brief period of half-light indicated by a white to black gradient. Traces are running averages over 30 mins. E) Representative histogram showing densities of resting HR values following i.p. injections of either saline (black) or 2 mg/kg CNO (magenta). Resting HR values after saline and CNO, respectively, were taken from hours 8.5-10.5 (1-2 hours post-injection) to avoid contamination of resting HRs with HR values during handling stress. Total density areas of individual histograms are 100. F, G) Change in resting HR (F) and percent of time spent active (G) of hM3Dq-expressing mice (n=3) in response to saline (black circles) and 2 mg/kg CNO (magenta circles). *p<0.05, paired t-test. H) Change in HR (mean±SEM) from baseline of urethane/ α -chloralose-anaesthetized mice in response to application of saline (n=7) or GLP-1 (0.4 μ g, n=7) directly onto the thoracic spinal cord. Two-way ANOVA: Drug x time $F_{(5, 55)} = 7.18$, p<0.0001, followed by Sidak's post-hoc multiple comparisons test (**p<0.01, ***p<0.001 vs saline). I) Change in HR (mean±SEM) from baseline of urethane/ α -chloralose-anaesthetized mice in response to application of Ex-9 (18.75 μ g, n=5), or by GLP-1 (0.4 μ g, n=5) 25 min after Ex-9, directly onto the thoracic spinal cord. Two-way ANOVA: Drug x time $F_{(5, 40)} = 3.971$, p=0.0051, followed by Sidak's post-hoc multiple comparisons test (**p<0.01 vs Ex-9). J) Change in HR 10 min after application of each drug. Ex-9 applied to the thoracic cord did not significantly change HR, but significantly reduced the effect of subsequently applied GLP-1. Two-way mixed model ANOVA: GLP-1 x Ex-9 $F_{(1,10)} = 5.525$, p=0.0406, followed by Sidak's post-hoc multiple comparisons test (*p<0.05).

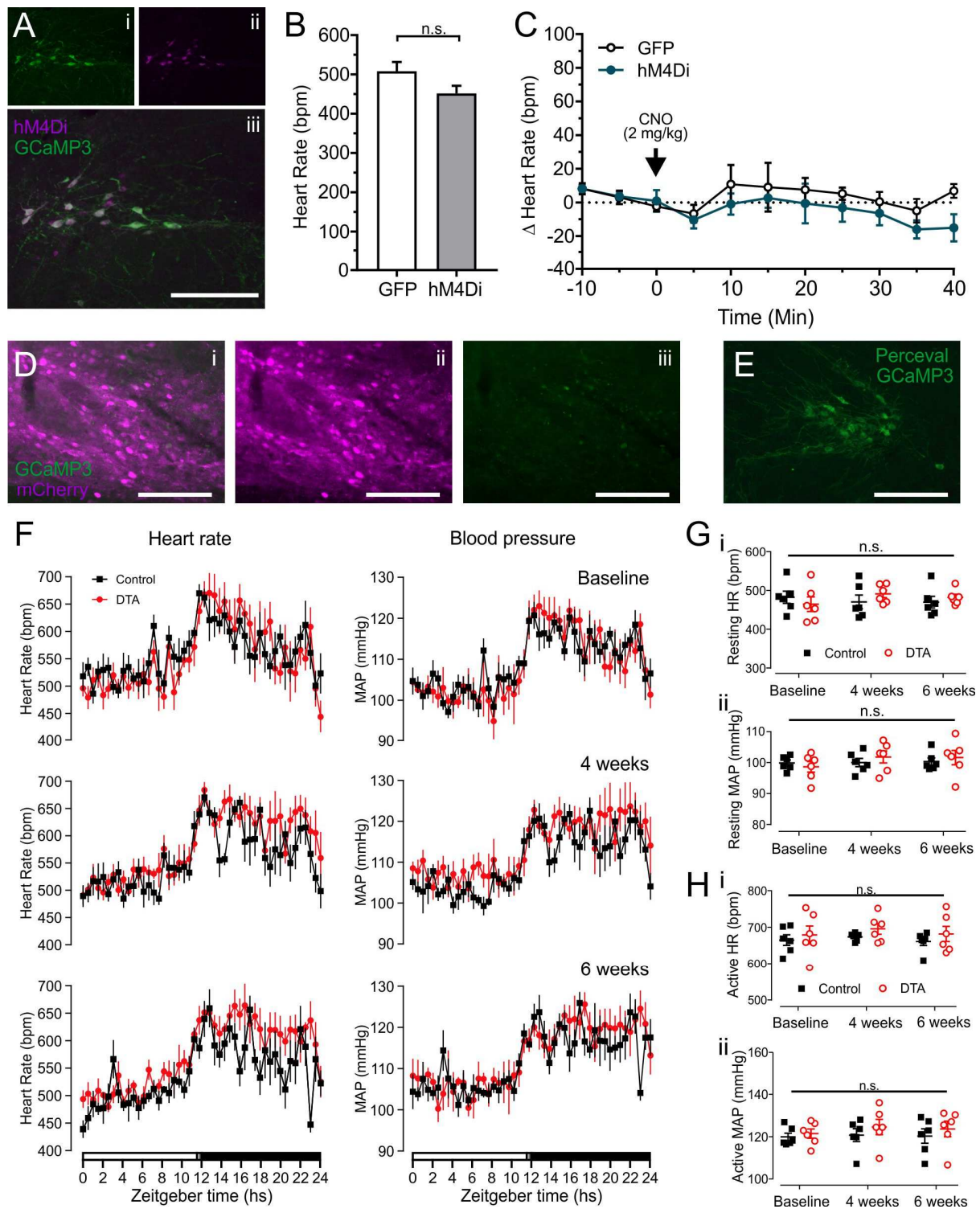


Figure 4: Ablation of PPG^{NTS} neurons does not affect HR or MAP under resting conditions

A) Representative images of immunofluorescence double-labelling of GCaMP3 (green, indicating PPG^{NTS} neurons) and hM4Di:mCherry (magenta) in the caudal NTS. B) HR at baseline for control (GFP) and hM4Di expressing mice prior to CNO administration. C) Change in HR from baseline of anesthetized mice expressing either GFP (n=5) or hM4Di (n=3) in PPG^{NTS} neurons selectively in response to CNO (2 mg/kg) injected at 0 mins (arrow). Virus x time: $F_{(8, 48)} = 0.196$, $p=0.9902$. D) representative photomicrographs of

immunofluorescence double-labelling of GCaMP3 (green, indicating PPG neurons) and mCherry (magenta) expressed cre-independently from AAV8-mCherry-FLEX-DTA in the caudal NTS. Note the presence of green fluorescent debris, much smaller than cell bodies, only. E) Representative image of immunofluorescence double-labelling of GCaMP3 and Perceval (both green) in the caudal NTS, indicating presence of PPG^{NTS} neurons in mice injected with control virus for ablation experiments. All scale bars: 200 μ m. F) HR (panels on left) and MAP (panels on right) were recorded before DTA ablation of PPG^{NTS} neurons (Baseline, top panel) and at four (middle panel) and six weeks (bottom panel) after surgery. Traces display mean \pm SEM HR and ABP every 30 mins for control (black squares; n=6) and DTA mice (red circles; n=6). Light (white bar), half light (gradient bar) and dark phase (black bar) are indicated at the bottom along with Zeitgeber time. G, H) Resting (G) and active (H) HR and MAP of control and PPG^{NTS}-DTA (DTA) mice at baseline, four weeks, and six weeks after surgery. n.s.: no significant interaction or main effects according to two-way mixed model ANOVA: Resting HR: Virus x time: $F_{(2, 20)} = 2.178$, $p=0.14$; main effects of virus ($p=0.78$) and time ($p=0.74$). Resting MAP: Virus x time: $F_{(2, 20)} = 1.522$, $p=0.2426$; main effects of virus ($p=0.77$) and time ($p=0.14$). Active HR: Virus x time: $F_{(2, 20)} = 0.0835$, $p=0.9202$; main effects of virus ($p=0.36$) and time ($p=0.37$). Active MAP: Virus x time: $F_{(2, 20)} = 0.1653$, $p=0.85$; main effect of virus ($p=0.43$) and time ($p=0.65$).

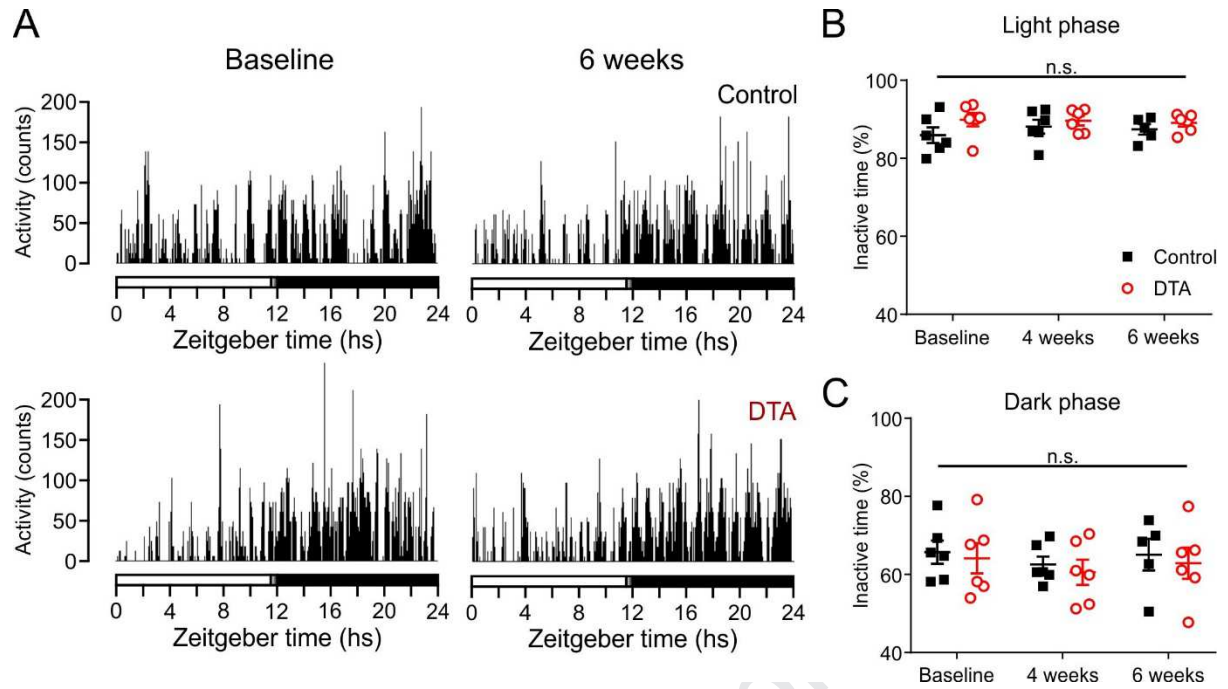


Figure 5: Ablation of PPG^{NTS} neurons does not affect locomotor activity or changes in HR in response to increased activity

A) Activity plots from representative control (top panels) and PPG^{NTS} -DTA (DTA, bottom panels) mice prior to viral injection (Baseline, left) and six weeks post-injection (6 weeks, right). B, C) Percent of time spent inactive of control (black squares) or PPG^{NTS} -DTA mice (DTA, red circles) during the light (B) and dark phase (C). Virus x time (light phase): $F_{(2, 20)} = 0.9748$, $p=0.39$; main effect of virus ($p=0.25$) and time ($p=0.71$). Virus x time (dark phase): $F_{(2, 20)} = 0.006161$, $p=0.9939$; main effect of virus ($p=0.65$) and time ($p=0.44$).

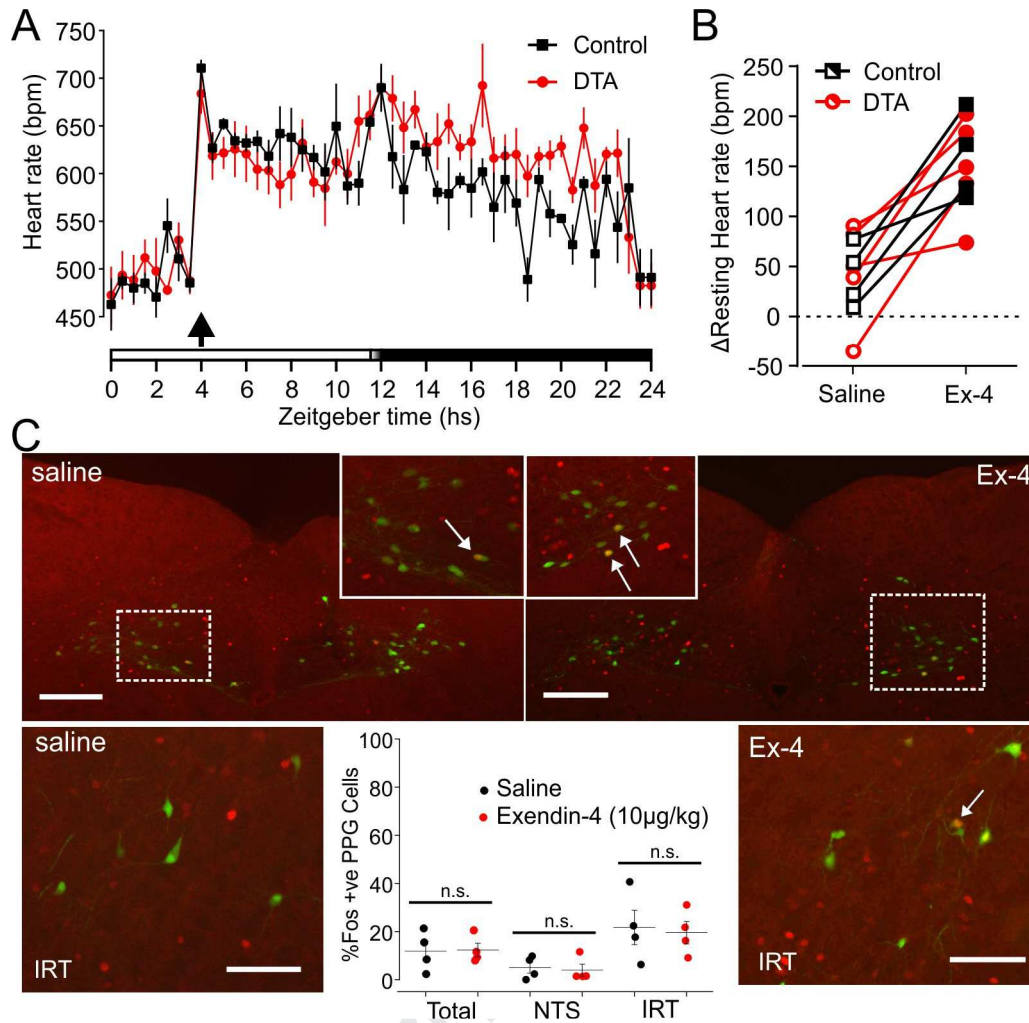


Figure 6: PPG^{NTS} neurons are not necessary for the tachycardic response to systemic GLP-1R activation

A) HR of control (black squares, $n=4$) and PPG^{NTS}-DTA mice (DTA, red circles, $n=5$) injected i.p. with 10 μ g/kg Ex-4 (red) four hours into light phase (arrow). Shown here are mean \pm SEM every 30 mins over 24 hours as indicated by zeitgeber time on the x-axis. The bar at the bottom indicate light (white bar) and dark (black bar) phases with a brief period of half-light indicated by a white to black gradient. B) Change in resting HR of control (black squares) and PPG^{NTS}-DTA mice (red circles) in response to saline (open symbols) and 10 μ g/kg Ex-4 (filled symbols). Drug \times virus: $F_{(1, 7)} = 0.3287$, $p=0.5844$; no significant main effect of transgene expression ($p=0.7610$), but a significant main effect of treatment ($p=0.0008$). C) Representative images and quantification of immunofluorescence labelling of cFos (red) in the caudal NTS (top panels) and IRT (bottom panels) following i.p. injection of saline or Ex-4 (10 μ g/kg). Green indicates native YFP immunofluorescence signal in PPG neurons. Scale bars: 100 μ m. Quantification plots show mean \pm s.e.m of % cFos-IR positive PPG neurons in NTS and intermediate reticular nucleus (IRT) for 4 mice under each condition. Unpaired t-tests revealed no significant differences between saline- and Ex-4-treated mice.

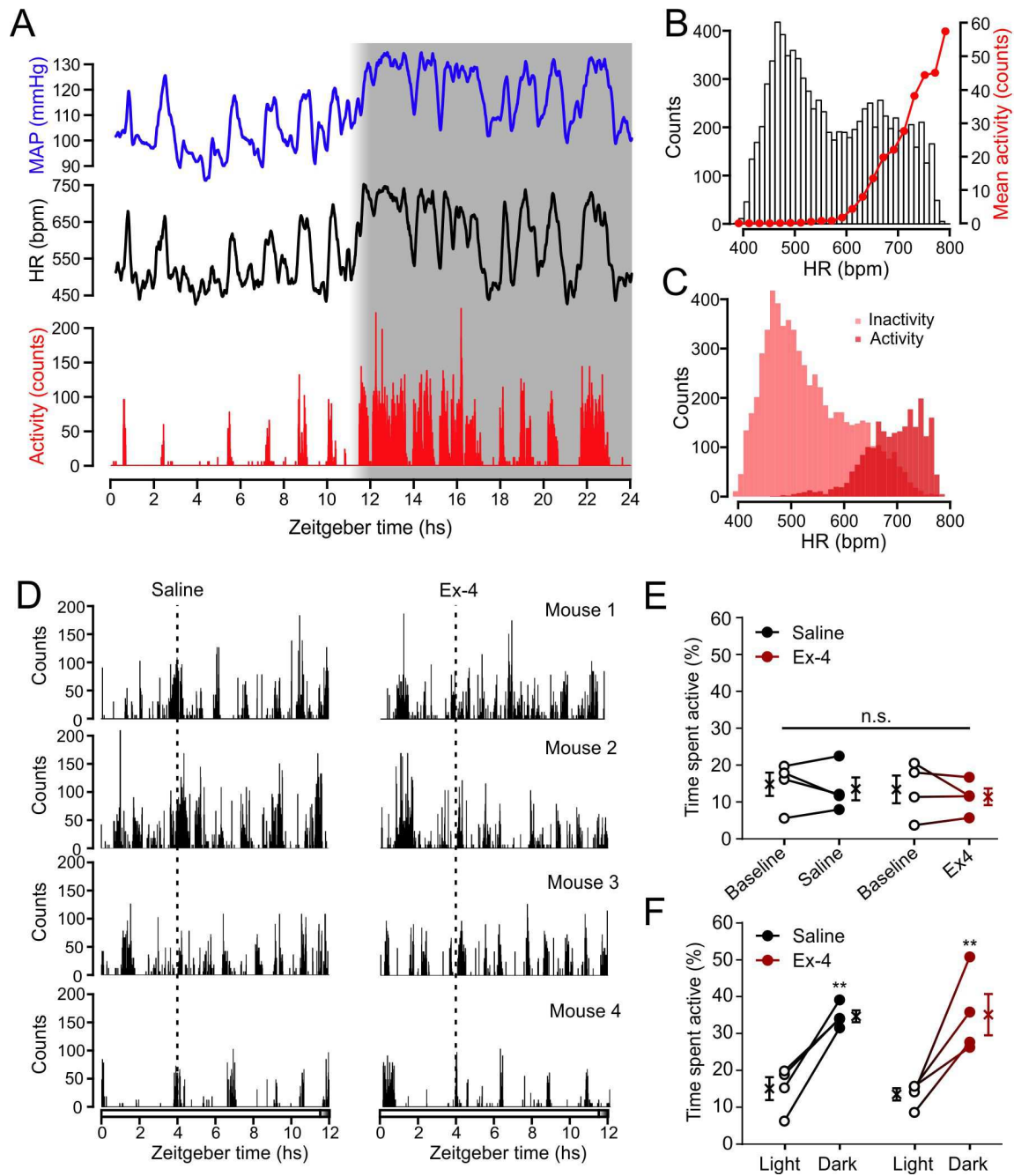


Figure S1: PPG^{NTS} neurons are not necessary for the tachycardic response to systemic GLP-1R activation

A) MAP (blue, top), HR (black, middle) and locomotor activity (red, bottom) measured from a single, naïve mouse over 24 hours as indicated in zeitgeber time. Dark phase is indicated with a grey box with the gradient indicating a half hour “twilight” period in which lights were dimmed. Traces are running averages over 20 mins. B) Histogram displaying the bimodal distribution of HR values in 10 bpm bins recorded from a single mouse over 24 hours. Overlaid in red are the mean activity counts at the HR levels indicated on the x-axis. At activity level 0, HR ranged between 390 and 570 bpm. At higher mean activity levels higher HR was associated with higher activity. C) The distribution of HR values from B) split into two histograms according to activity levels with the distribution of HR values at inactivity (when activity=0) displayed in light red, and the distribution of HR values during active times

in dark red. Importantly, neither distribution was normal with inactive HR values skewed to the right and active HR values skewed to the left. For this reason, estimates of resting and active HR and MAP values for individual mice implanted with biotelemetry probes are all based on the median. D) Activity levels of naïve mice (n=4) implanted with biotelemetry probes and injected i.p. with saline (left) or 10 µg/kg Ex-4 (right) four hours into light phase. Activity levels were monitored over 12 hours during light (white bar) and twilight phase (gradient bar). Zeitgeber time is indicated at the bottom. Times of i.p. injections with either saline or Ex-4 are indicated with dotted lines. E) Percentage time spent active before (Baseline, hours 1-4, open circles) and after (Saline/Ex-4, hours 5-8, filled circles) i.p. injection of saline (black) or 10 µg/kg Ex-4 (red) four hours into light phase. Drug x time: $F_{(1, 3)} = 0.034$, $p=0.87$; main effect of time ($p=0.29$) and drug ($p=0.39$). F) Percentage time spent active during light (open circles, hours 8-11) and dark phase (filled circles, hours 12-15) following injection of Ex-4 (10 µg/kg) four hours into light phase. Drug x time: $F_{(1, 3)} = 0.096$, $p=0.78$; no main effect of drug ($p=0.83$), but a significant main effect of time (** $p=0.0058$).

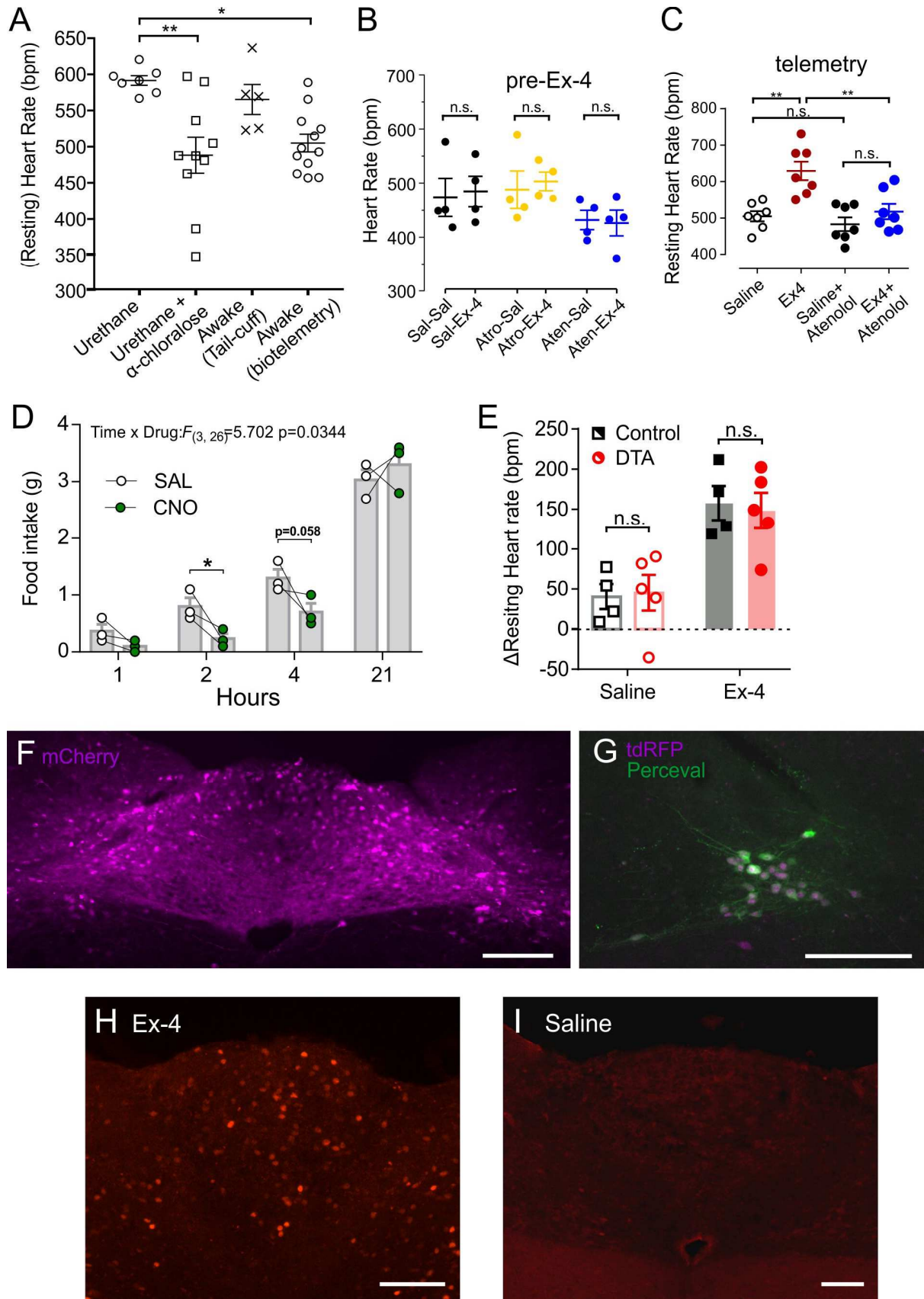


Figure S2:

A) Resting HR under two types of anaesthesia and in awake animals using either tail-cuff measurements with restraint or biotelemetry blood pressure probes in freely behaving mice.

One way ANOVA: $F_{(3, 31)} = 5.812$, $p=0.0028$ followed by Tukey's post-hoc tests (* $p<0.05$, ** $p<0.01$) B) HR in mice injected i.p. with saline, atropine (2 mg/kg), or atenolol (2 mg/kg) prior to injection with either saline or Ex-4 as indicated. Unpaired t-test revealed no significant differences as indicated by n.s. C) HR in freely behaving mice injected i.p. with Ex-4 (10 $\mu\text{g}/\text{kg}$) or saline in the absence or presence of atenolol (2 mg/kg). $n=7$. D) Cumulative food intake of mice expressing hM3Dq in PPG^{NTS} neurons selectively during the dark phase following i.p. injection of CNO (2 mg/kg, $n=3$). Drug \times time: $F_{(3, 6)} = 5.702$, $p=0.034$; * $p<0.05$ according to Sidak's multiple comparisons test. E) Change in resting HR of control (black squares) and PPG^{NTS}-DTA mice (red circles) in response to saline (open symbols) and 10 $\mu\text{g}/\text{kg}$ Ex-4 (filled symbols). Treatment \times virus $F_{(1, 7)} = 0.3287$, $p=0.5844$; no main effect of virus ($p=0.7610$), but a significant main effect of treatment ($p=0.0008$). F) Representative image of mCherry (magenta) fluorescence expressed cre-independently from AAV8-mCherry-FLEX-DTA in the caudal NTS indicating spread of virus after stereotaxic injection. Scale bar: 200 μm G) Representative image of immunofluorescence double-labelling of tdRFP (magenta, indicating PPG^{NTS} neurons) and Perceval (green) in the caudal NTS demonstrating successful transduction by control AAV. Scale bar: 200 μm . H, I) Intraperitoneal injection of Ex-4 (10 $\mu\text{g}/\text{kg}$; F), but not saline (G) induced C-Fos-IR in the area postrema. Scale bars: 100 μm .

Highlights

- Activation of PPG neurons triggers increases in heart rate in mice
- PPG neurons do not provide a tonic sympathetic drive to the heart
- The tachycardic effect of systemic Ex-4 is not mediated by PPG neurons
- GLP-1 receptor activation has a sympathoexcitatory effect that raises heart rate
- Local activation of GLP-1R in the spinal cord is sufficient to elicit tachycardia

Journal Pre-proof

Declaration of interests

The authors declare that they have no known competing financial interests or personal relationships that could have appeared to influence the work reported in this paper.

The authors declare the following financial interests/personal relationships which may be considered as potential competing interests: